INFORMATION TO USERS

This manuscript has been reproduced from the microfilm master. UMI films the text directly from the original or copy submitted. Thus, some thesis and dissertation copies are in typewriter face, while others may be from any type of computer printer.

The quality of this reproduction is dependent upon the quality of the copy submitted. Broken or indistinct print, colored or poor quality illustrations and photographs, print bleedthrough, substandard margins, and improper alignment can adversely affect reproduction.

In the unlikely event that the author did not send UMI a complete manuscript and there are missing pages, these will be noted. Also, if unauthorized copyright material had to be removed, a note will indicate the deletion.

Oversize materials (e.g., maps, drawings, charts) are reproduced by sectioning the original, beginning at the upper left-hand corner and continuing from left to right in equal sections with small overlaps.

ProQuest Information and Learning
300 North Zeeb Road, Ann Arbor, MI 48106-1346 USA
800-521-0600

REVISITING HEMODYNAMIC ANALYSIS OF PULMONARY EDEMA AFTER THE ONSET OF LEFT VENTRICULAR DYSFUNCTION USING A MATHEMATICAL MODEL OF THE CARDIOVASCULAR SYSTEM.

SHALINI VEERASSAMY
Department of Biomedical Engineering
Faculty of Medicine
McGill University
Montreal, Quebec

November 2000

"A thesis submitted to the Faculty of Graduate Studies and Research in partial fulfillment of the requirements of the degree of Masters of Engineering (M.Eng)"

CONTENTS

List of Figures:

List of Tables:

Acknowledgments

I would like to thank my supervisors namely Dr. Jason Bates, Dr. Henrietta Galiana and Dr. Sheldon Madger for their support and guidance throughout my stay at the Biomedical Engineering Department, Mcgill University. I would like to thank my parents, Dr. Deva and Ruby Veerassamy and sisters for their continuous encouragement and support. I would like to thank all the students and staff of the department who have contributed in my being able to attain this goal.

This work was supported by operating grants from the Medical Research Council (MRC) of Canada.

ABSTRACT

The aim of this project was to extend a mathematical model of the cardiovascular circulation, originally built by Burkhoff and Tyberg [6]. The model was implemented in Simulink and consists of 6 lumped vascular compartments interconnected by segments allowing unidirectional blood flow. A set of 6 differential equations describe changes in blood volume in the four systemic and two ventricular compartments as functions of time in terms of the pressure across each compartment and the resistances between them. The model was used to investigate why pulmonary venous pressure rises after the onset of left ventricular dysfunction. Special attention was given to the pericardial and peripheral resistance effects. Sensitivity analysis showed that our parameter values and ratios were more appropriate than those of Burkhoff and Tyberg [6]. We conclude that, although stressed volume has a fundamental role in raising the pulmonary venous pressure, contractile strength and systemic arterial resistance also contribute considerably.

EXTRAIT

Le but de ce projet était de mettre au point un modèle mathématique de la circulation cardiovasculaire, conçue à l'origine par Burkhoff et Tyberg. Ce modèle a été implémenté sur Simulink et consiste en 6 compartiments vasculaires interconnectés par des branches qui laissent passer le flot unidirectionel de sang. Un ensemble de 6 équations différentielles décrivent les modifications du volume sanguin dans les 4 compartiments systémiques et les 2 compartiments ventriculaires. Le modèle a été utilisé dans le but de voir pourquoi la pression de la veine pulmonaire croît après le début de la dysfonction du ventricule gauche. Des observations plus poussées ont identifié des effets de résistance du péricarde et de la périphérie. Des analyses de sensibilité ont démontré que les valeurs et ratios de nos paramètres étaient plus appropriés que ceux de Burkhoff et Tyberg. Nous concluons donc que même si le volume du stress joue un rôle majeur dans la montée de la pression de la veine pulmonaire, la force contractile et la pression systémique artérielle y contribuent aussi considérablement.

INTRODUCTION

The aim of this project was to extend a mathematical model of the heart and circulation originally developed by Burkhoff and Tyberg [7] in order to investigate hemodynamic determinants of cardiac output. The revised model was implemented in MATLAB using Simulink 3.0. The model consists of 6 compartments; a right and left heart, lumped pulmonary artery and vein compartments and lumped systemic artery and vein compartments. The compartments are interconnected by segments allowing unidirectional blood flow. A set of six differential equations describes changes in blood volume in the 4 systemic and 2 ventricular compartments as functions of time in terms of the pressure across each compartment and the resistances between them. The right and left ventricular pumping characteristics are represented by time-varying elastances theory that relate instantaneous ventricular pressure to volume.

The revised model is used to re-assess the importance of decreased ventricular contractile state, increased heart rate, increased arterial resistance and decreased venous capacity in the development of pulmonary congestion after the onset of acute Left Ventricular Dysfunction (LVD). The model parameter values were chosen according to Magder [24]. We considered the effects of changes in pericardial mechanics, systemic venous resistance, the baroreceptor reflex and sepsis on Pulmonary Venous Pressure (PVP) after LVD.

A sensitivity analysis of the model was performed by perturbing each of the parameters in turn by $\pm$ 5% and observing the changes in cardiac output and the various compartmental pressures.

ORGANIZATION OF THE THESIS

Chapter 2 gives an overview of circulatory mechanics, starting with the systemic and pulmonary circulations. The relationships between volume, pressure and flow are discussed. Systemic and pulmonary resistances and compliances are reviewed. Modeling objectives, methodology and classification are also considered in this chapter, which closes with the historical origins and uses of the different levels of modeling.

Chapter 3 reviews some key models developed for use in cardiovascular research. The chapter starts with a short historical review and then focuses in more depth on particular models. The model equations are described in detail along with schematic representations.

Chapter 4 deals with the basic structure and equations involved in the model developed in the present study. A set of six differential equations describing how volume changes in each compartment is given. The right and left hearts are represented by time-varying elastances. The Burkhoff and Tyberg model is compared to its extension developed herein. The chapter also gives a brief description of the Simulink software that was used to implement the model.

Chapter 5 establishes the control parameter values used in the model. The effects of changing heart rate, LV end systolic elastance, systemic arterial resistance, and stressed volume and their role in influencing LVD is investigated. The effects of changes in

systemic venous resistance on its own, with the inclusion of the baroreceptor reflex and with sepsis are also investigated. A sensitivity analysis is also performed.

Chapter 6 describes the results achieved with the model. Limitations of the Model, and suggestions for future research are also presented.

CHAPTER 1

BACKGROUND

1.1 Introduction

The cardiovascular system is the main transport system of the body. A model of an individual's cardiovascular system must imitate the relationships among physiological variables, such as heart rate, systolic and diastolic blood pressures, and breathing rate, at different physical activity levels. There are four basic types of models used in medicine: non-mammalian models, culture models, mammalian models and mathematical, computer and physical models.

1.2 Types of Models

(1) Non- mammalian models

Non-mammalian models are a species that can serve as excellent models for certain biological processes and structures, and are indispensable in the study of others. For example the giant axon of the squid was the key experimental system at the birth of modern neuroscience. Nevertheless, inter-taxonomic transfer of information should be approached with great caution because species difference can be great or even, as in embryonic development, fundamental.

The advantages of non-mammalian models are:

(1) generally they are more readily available and less expensive than mammals,

(2) the processes they are supposed to illustrate are often displayed more simply and directly than in higher animals,

(3) their tissues and organs are more accessible and may lend themselves more easily to microscopic observation, dissection, and laboratory handling.

Some limitations of non-mammalian model include that unless some fundamental similarity to the human system under study is established, the results cannot be reliably applied to the human system.

(2) Culture models

Culture models involve the culture of cells, tissues and organs, including those of human origin, and have attained a high level of sophistication. They have been responsible for many recent discoveries. The strengths of this technique are that the cells and tissues in culture can be maintained in a defined, controlled environment, provided they retain the differentiated functions that existed in the whole-body system. They are also capable of providing a rapid and less expensive means of evaluating physical and chemical agents than live animals, and have allowed the discovery of information that would not have been obtainable from research on more complex systems. Limitations include the fact that cultured cells may lose their differentiated function, and they may not mimic the in-vivo response because of the absence of complex tissue and organ interactions that ordinarily give rise to it. Also, a particular behaviour may be due to infection of the culture by an unknown and undetected pathogen.

(3) Mammalian models

From historical record, it is clear that mammalian models have been central to the development of modern medicine, both for understanding normal physiology and for developing diagnoses and therapies. This centrality continues, and for many subtle and long-term effects of drugs or therapies there is no alternative. Some of the strengths of mammalian models are that humans are mammals. Furthermore mammalian models in

which disease development and response to therapy are similar to those in humans can very often be found. Mammalian models provide standardized and federally mandated methods for testing the safety and efficacy of new drugs before they are released for human clinical trials. Finally mammalian models offer the only reliable testing for complex prostheses or interventions in which the collective response of the whole system is important.

Some of the limitations of mammalian models include species differences in details of anatomy and physiology so that similarity of test mammalian species to human systems must be established before results can be generalized. Also, some otherwise desirable mammalian models may be expensive and difficult to acquire and maintain.

(4) Mathematical computer and physical models

Mathematical models and computer simulations are finding increased use and application as the available computing power increases. The advantages of such models are:

(1) they codify facts and help confirm or reject hypotheses about complex systems,

(2) they reveal contradictions or incompleteness of data and hypotheses,

(3) they can often allow prediction of system performance under untested or untestable conditions,

(4) they can predict and supply the values of experimentally inaccessible variables,

(5) they suggest the existence of new phenomena.

Some of the limitations are:

(1) the selection of model elements may be suboptimal,

(2) incorrect models can fit limited data, leading to erroneous conclusions,

(3) simple models are easy to manage but complex models could be needed,

(4) realistic simulations often require a large number of parameters, and the values needed could be very difficult to obtain.

Mathematical models are good when there is sufficient knowledge of the system to allow the formulation of strong hypotheses. As the sophistication of computing increases, and as our ability to acquire data expands, more effective and broader applications may be expected. The limitations of prediction due to system complexity remains, but further advances are to be anticipated with confidence. Physical models are similar in their strengths and weaknesses to computer models. However, at present they are more limited in their ability to represent the complex interactions that occur within living systems accurately.

Cardiac mechanics and hemodynamics lend themselves readily to mathematical and computer modeling. Therefore the achievements to date and the prospects of future research in this area provide an example of the potential of mathematical and computer modeling. When involved in computer studies of blood flow in the heart, the normal function of the heart can be elucidated, and diseases that influence the mechanical function of the heart can be examined.

1.3 Application of cardiovascular models

Models are indispensable for biomedical research. There is no branch of medicine or life science in which the current knowledge base is not determined in some way by research with models. A model of the cardiovascular system originally formulated by D. Burkhoff and J. Tyberg [7] forms the basis of the current project.

Application of cardiovascular models lies mainly in the areas of research and clinical medicine. The purpose is typically to investigate the response of the intact circulation to various perturbations, which is intuitively difficult due to the nonlinear feedback nature of the system. The effects of Central Nervous System (CNS) control and cardiovascular drugs may also be incorporated. There seems to be a tendency for many cardiovascular models to be 'comprehensive' so that a wide range of situations can be modeled. Such models, for instance Beneken and De Wit 1967; Pullen 1976 etc., will be discussed in the later chapters. The major difficulty with such models is validating them.

1.4 Heart Failure

When the heart is unable to pump blood in sufficient amounts to meet the metabolic requirements of the tissues of the body, a complex series of derangements happen throughout the cardiovascular system. These in turn cause widespread disturbances of body functions. These perturbations become apparent to the clinician as the signs of heart failure and lead to the symptoms perceived by the patient. Circulatory failure can sometimes occur in the presence of an increased cardiac output, reflecting the inability of

the heart to maintain a normal cardiac output. However, in most cases the heart failure is due to changes in the heart muscle itself.

1.4.1 Hemodynamic Changes

When pumping action of the left ventricle is impaired, end-diastolic pressure increases causing a retrograde increase in left atrial and pulmonary vein pressure. As the left atrium dilates, the posterior cusp of the mitral valve is retracted causing mitral regurgitation, and the pulmonary vessels overfill with blood. The ensuing rise in pulmonary capillary hydrostatic pressure causes interstitial edema followed by exudation of fluid into the alveoli (pulmonary edema). As the pulmonary pressure increases the work of the right ventricle is raised leading to overload and eventual right ventricular failure. When the right ventricle fails, there is an increase in right ventricular and right atrial pressure, which lead to dilatation of the tricuspid atrioventricular ring and tricuspid incompetence. As the atrial pressure rises the systemic veins become engorged and peripheral edema ensues.

Thus, one of the most common and important consequences of acute LVD is pulmonary edema, which results from a rise in pulmonary venous pressure.

CHAPTER 2

OVERVIEW OF CIRCULATORY MECHANICS

2.1 Introduction

The cardiovascular system is the main transport system of the body. The system transports respiratory gases, nutrients, and wastes to and from cells. The main components of the cardiovascular system are:

(1) heart

(2) arteries

(3) veins

Heart: The human heart has 4 chambers; two-thin walled atria separated by an interatrial septum, and two-thick walled ventricles separated by an interventricular septum. The heart has 4 valves; the mitral, tricuspid (atrioventricular) and the pulmonary, aortic (semilunar valves). The mitral and tricuspid valves open to allow blood to fill the ventricles when the blood pressure is low and velocity is small. The mitral and tricuspid valves are attached to papillary muscles which contract during systole and, pull down the valves to generate systolic pressure rapidly and prevent the valves from inverting into the atrium. The aortic and pulmonary valves are used in ventricular systole to pump blood out of the ventricles at high velocity. Unlike the mitral and tricuspid valves, the semilunar valves have no strings attached. The opening and closing of all valves are operated by blood itself through hydrodynamic forces.

Arteries: Arteries are thickly walled, muscular, elastic tubes whose diameters vary with pulsatile pressure. The arterial wall belongs to the class of materials called visco-elastic, exhibiting properties appropriate to both an elastic solid and a viscous liquid. These

vessels conduct oxygenated blood away from the heart to the lungs with the exception of the pulmonary arteries which channel the deoxygenated blood from the heart to the lungs.

Veins: Veins are relatively thinly walled, highly compliant, collapsible, large-capacity vessels with relatively low transmural pressures and non-linear modeling has to be applied to obtain an adequate representation of them. Valves are located at various locations in the venous system to ensure unidirectional blood flow. These vessels direct deoxygenated blood towards the heart with the exception of the pulmonary veins, which carry oxygenated blood from the lungs to the heart. Venules, which are small veins, collect blood from the downstream end of the capillary beds. Large veins channel blood from the main venous branches to the vena cava, and flows into the right heart.

Heart Cycle: In a normal adult, heart rate is about 75 beats per minute. Diastole is the period of ventricular relaxation when blood fills the ventricle and systole is the period of ventricular contraction. The P-wave signals the start of electrical stimulation of the heart muscle and in about 0.1 seconds, as the excitation spreads over most of the atrial muscle, atrial contraction begins causing a single increase in both atrial and ventricular pressures. This rise in pressure happens in both cardiac chambers because the atrio-ventricular (mitral and tricuspid) valves are open. In the late stage of diastole the ventricles are invaded by electrical excitation process as it spreads over the atrial muscle from the SA (sino-atrial) node via the bundle of His and the Purkinje fibres. Ventricular contraction starts not long after the onset of the QRS complex. The ventricles begin to contract; the intra-ventricular pressure begins to rise, causing the AV (atrio-ventricular) valve to close (first heart sound). This period of ventricular contraction lasts about 0.05 seconds and is called the 'isovolumic phase of contraction' (isovolumic because the ventricles are

isolated and the volume remains constant). The contraction phase continues and the intra-ventricular pressure rises rapidly until it exceeds the pressures in the pulmonary artery and aorta. Then the semilunar valves open and systole starts. Blood is expelled from the ventricles. At first, ejection is fast and then declines during the later stage of systole. The period of ventricular systole lasts about 0.3 seconds after which the ventricles start to relax and their pressures drop rapidly closing the aortic and pulmonary valves (second heart sound). The isovolumic relaxation phase continues for about 0.08 seconds after the semilunar valves close. The relaxation phase ends with the opening of the AV valves, which occurs when ventricular pressures fall below atrial pressures. When the AV valves open, a phase of rapid filling starts. Blood accumulates in the atria during systole and elevates their pressures. When ventricular pressures drop below atrial pressures, blood rushes down the pressure gradient between atrium and ventricle. This phase of rapid filling lasts about 0.1 seconds. The final stage of the cardiac cycle is known as the phase of slow filling or diastasis. This period lasts about 0.2 seconds and is due to continued venous return and is terminated by atrial systole.

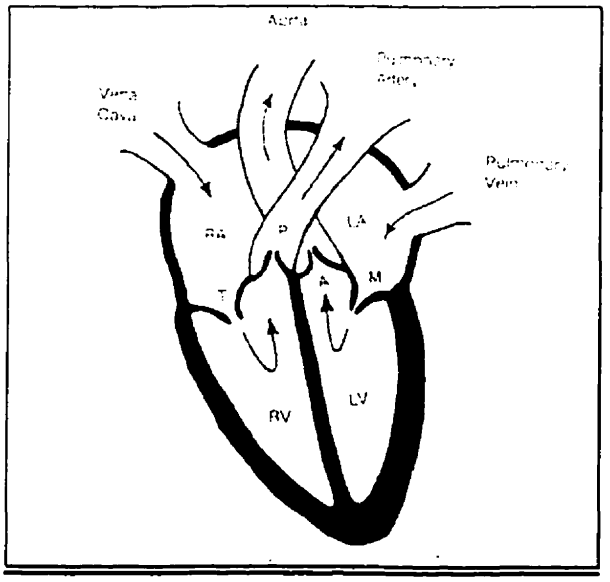

Figure (1) Representation of the heart [6].

2.2 Pattern of circulation

The circulatory system, a continuous network of blood vessels, is divided into two sub-systems known as the systemic circulation and the pulmonary circulation. Blood is pumped by the left ventricle into the systemic circulation, which channels oxygenated blood to all the different organs and tissues. Deoxygenated blood returns to the right atrium of the heart and is pumped by the right ventricle into the pulmonary circulation. The pulmonary arteries channel blood to the lungs where gas exchange occurs. Blood, rich in oxygen, is then returned by the pulmonary veins to the left atrium. Blood passes into the left ventricle and is again pumped into the systemic circulation, thus repeating the double cycle.

2.2.1 Systemic circulation

Blood returning to the heart from the pulmonary circulation is oxygenated. It enters the left atrium then passes into the left ventricle from which it is pumped into the aorta, the largest artery in the body. The part of the aorta that travels upwards is called the ascending aorta. The ascending aorta branches into coronary arteries which enter the heart muscle. The aorta, after a short distance, makes a U-turn called the aortic arch. The three large arteries that branch off from the aortic arch are:

(i) the brachiocephalic artery supplying the right upper portion of the body.

(ii) the left common carotid artery supplying the left side of the head and neck

(iii) the left subclavian artery supplying the neck and left arm.

The descending aorta is that part of the aorta passing down through the thoracic and abdominal cavities. The abdominal aorta is reaching below the diaphragm. Branches

from the aorta are channeled to all major organs and tissues. For example, the renal arteries branch off to the kidneys. The left and right common iliac arteries are divisions of the aorta in the lower abdominal cavity. They deliver blood to the lower extremities and pelvic structures.

Blood returns to the heart via two large veins, the superior and inferior vena cava. The inferior vena cava receives blood from the portion of the body below the level of the diaphragm. Two brachiocephalic veins collect blood from the upper portion of the body and empty it into the superior vena cava.

2.2.2 Pulmonary circulation

Blood returning to the heart from the systemic circulation is deoxygenated. The blood enters the right atrium, then the right ventricle from which it is pumped into the pulmonary trunk, a very large artery. The pulmonary trunk divides almost immediately into from the right and left pulmonary arteries. These vessels channel blood to the right and left lungs respectively. In the lungs, each pulmonary artery gives rise to branches that supply all regions of the organ.

Blood flows into the extensive capillary networks in the walls of the pulmonary alveoli, where oxygenation of blood occurs. Pulmonary capillaries deliver this blood to pulmonary venules which in turn join to form larger and larger veins. Two pulmonary veins exit from each lung and channel oxygenated blood to the left atrium of the heart. One should note that pulmonary veins are the only veins that carry oxygenated blood, and

that pulmonary arteries are the only arteries that carry deoxygenated blood. Below is a schematic representation of the circulatory system.

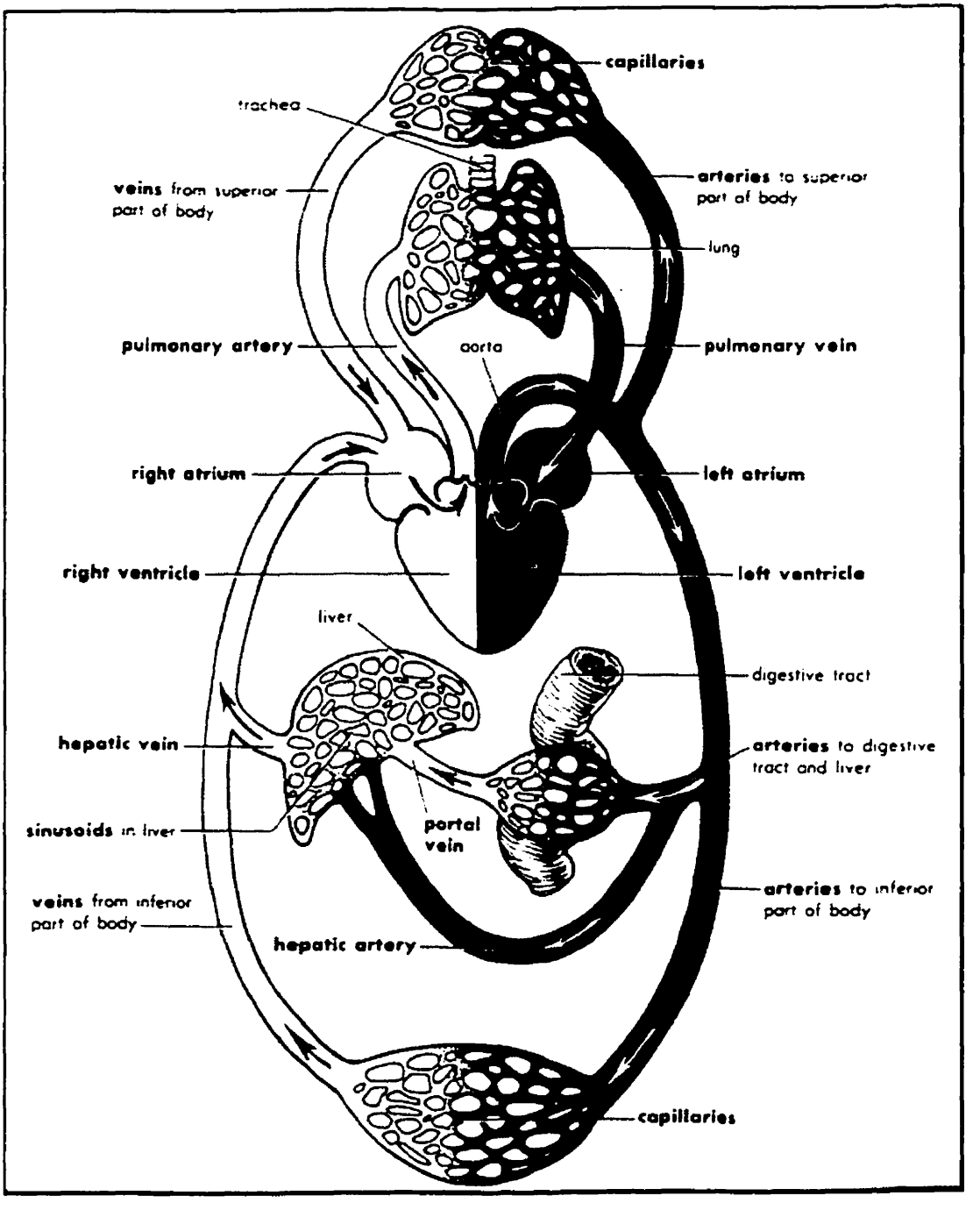

Figure (2) schematic representation of the circulatory system [12].

2.3 Volume–pressure relationships

The systemic and pulmonary blood vessels, like numerous other structures in the body, are elastic structures. The fundamental property of an elastic structure is its inherent ability to offer resistance to a stretching force and to return to its resting or unstressed length or volume after the stretching force has been lifted. The deforming stress is an increase in the intravascular fluid volume in the intact body. Such increases in the vascular volume will stretch the wall of the vessels and the recoil of the elastic vessel walls will increase the intravascular pressure. The ratio of the change in volume to the change in pressure is called compliance. Most physiologists prefer to define elastic behavior in terms of compliance even though the term elastance is extremely descriptive. Compliance is defined as the reciprocal of elastance.

$$C = \frac{V - V_u}{P} \qquad (2.1)$$

Where V_u is the resting (unstressed volume), that is the volume contained within the compliant structure when the pressure, P, within the compliant structure is zero, and V is the volume above the unstressed volume.

Below is an illustration of the volume-pressure relationships that are obtained when compliance (1/elastance) is changed.

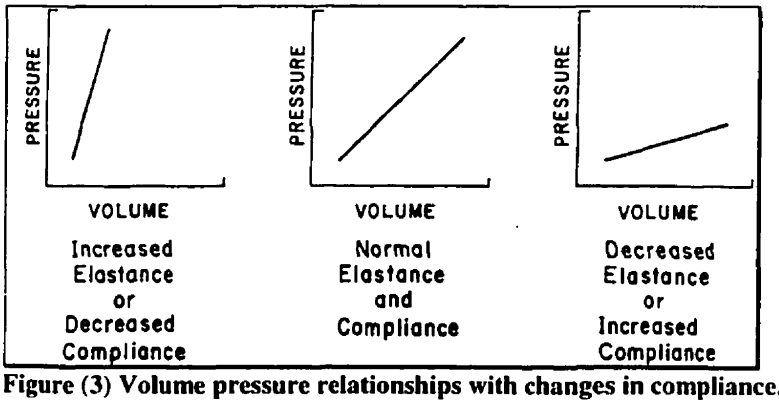

Figure (3) Volume pressure relationships with changes in compliance.[12]

2.4 Pressure- Flow relationships

The physical principles governing the flow of fluids through conducting passages (rigid or collapsible vessels) are derived from the general laws of hydrodynamics. The fluid can be either liquid such as blood flowing through the cardiovascular system, or air. The difference lies in the densities and viscosities of these fluids. The basic expression for the flow of liquid through rigid tubes is Poiseuille's law. Their law states that the volume of fluid flowing past a point in the tube per unit time (F) is proportional to the difference in pressure between the inflow and the outflow ends of the tube (Pi-Po) and the fourth power of the radius (r) of the tube, and inversely proportional to the length of the tube (l) and viscosity of the fluid (η).

Poiseuille's law can be expressed as follows for conditions of horizontal flow:

$$(Pi-Po)/F = 8\,\eta\, l/\pi\, r^4 \qquad (2.2)$$

The term on the right-hand side represents those factors which tend to retard flow and is known as the resistance to flow. The most commonly used relationship is therefore $(Pi-Po)/F=R$, where R is the resistance.

2.5 Systemic and Pulmonary Vascular Compliance

The total lumped compliance of the systemic circulation (i.e. of arteries, capillaries and veins) can be determined in experimental animals by momentarily stopping the circulation, then rapidly equalizing the arterial and venous pressures by pumping blood from arteries to veins (Guyton 1973, Green 1979). The intravascular pressure measured when arterial and venous pressures are equal is the static transmural pressure of the system at that blood volume and is also known as the mean systemic pressure (P_{ms}).

Pulmonary vessels, similar to those in the systemic circulation, are elastic, but with quantitatively different compliances. Most authors believe that the pulmonary arterial system (e.g. pulmonary artery) is more compliant than the systemic arterial system (e.g. aorta). Yet, when the lumped compliance of the pulmonary system (i.e. arteries, capillaries and veins) is compared with the lumped compliance of the systemic system, the pulmonary system is found to be considerably less compliant than the systemic bed. The compliance of the serial portions of the pulmonary bed is distributed differently from that of the systemic circulation. The compliance of large pulmonary arteries and veins are approximately equal (accounting to 15% of the total pulmonary vascular compliance). The small pulmonary vessels, small veins, venules and capillaries account for the rest of the pulmonary vascular compliance. Thus, it can be seen that blood vessels of both the systemic and pulmonary circulations are elastic structures and recoil inwardly when a volume stress is applied. The total compliance of the systemic circulation is greater than that of the pulmonary circulation. Also the venous systems of both circulations possess the greatest compliance.

2.6 Systemic and Pulmonary Vascular Resistance

In most physiological systems, an increase in the resistance to flow is interpreted as a decrease in the radius of the conduit(s) through which the flow occurs because the length and viscosity tend to remain constant. The blood pressure that develops in the arterial vessels of the systemic and pulmonary circulations is largely dissipated by the time the blood arrives in the atria. This fact indicates that the blood vessels have a resistive function in addition to their capacitive function. However, the magnitude of their resistance is different at different levels of the circulation. The ratio of driving pressure to

flow is called vascular resistance. At normal cardiac output of 5.0 l/min for an adult human, the mean systemic arterial pressure* is between 90-100mmHg. In the systemic circulation, the major pressure drops and thus the major resistance occurs upstream of the veins (in the arteries). On the other hand, at a normal cardiac output of 5.0 l/min, the mean pulmonary artery pressure is 8-15 mmHg. Unlike the systemic circulation, the distribution of vascular resistance in the pulmonary system is divided approximately equally between artery and veins. The total pulmonary vascular resistance is considerably less than the total resistance across the systemic bed.

2.7 Modeling in Physiology

2.7.1 Modeling objectives

The general categories of modeling objectives are normally identified as descriptive, predictive and explanatory. Descriptive modeling expresses the quantitative relationships in terms of equations. Predictive modeling determines how a system would respond to a stimulus or change in the system. Explanatory modeling is used for description of the ways in which different parts of the system behave and depend upon each other.

* Mean systemic arterial pressure v/s Mean systemic pressure. The former is the mean pressure in the systemic arteries whereas the latter is the pressure observed throughout the systemic circulation when cardiac output is zero.

2.7.2 Modeling methodology

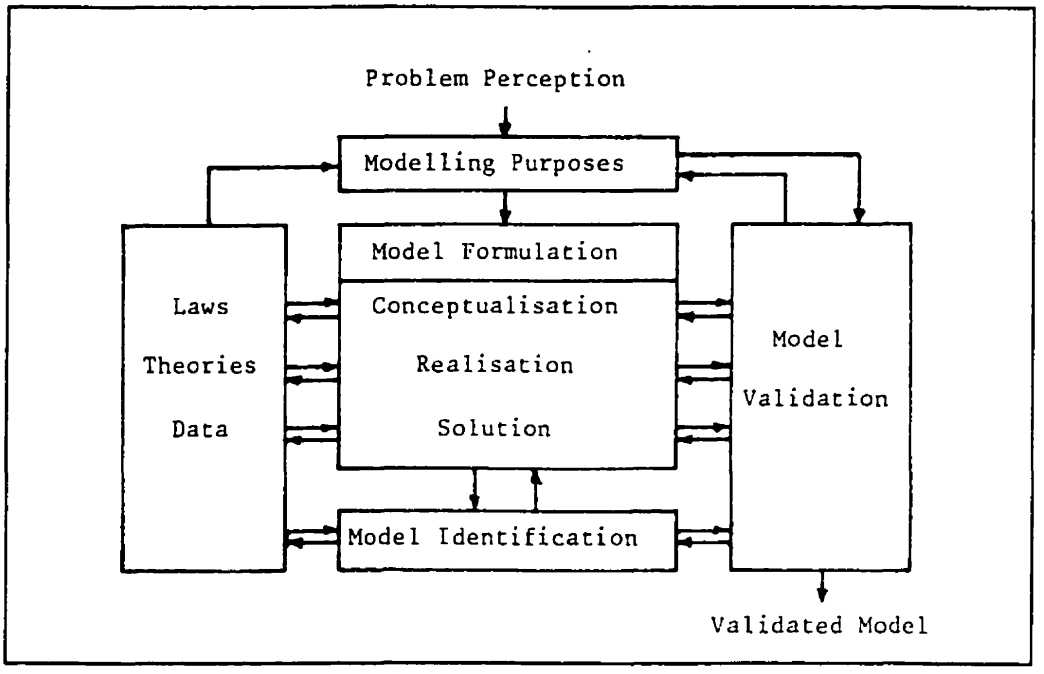

Figure (4) Distinct stages in the modeling process (Carson et al. 1983)

The above figure shows the different stages and information required in the modeling process. First there is the perception that a mathematical model will be useful. This could stem from a practical problem or theoretical inadequacies in background knowledge. Next follows the process of model formulation which involves conceptualization, realization, synthesis and solution. When the basic form of the model has been determined, identification may be used in some cases to resolve uncertainties, such as structural ambiguity or unknown parameters. The laws, theories, models and data form part of the background knowledge that is required throughout the process. Model validation is comprised of the application of a series of tests or critical assessments underpinned by specific validity criteria.

2.7.3 Model classification

Circulatory models can be classified into four levels of increasing complexity. The first and simplest model classification is the pure resistance model giving mean, continuous flow where pulsatile effects of blood flow are ignored. The second level of classification is the lumped (windkessel) model consisting of circulatory subsystems of discrete resistance, compliance and inertial effects. The third model classification is the distributed linear model in which circulatory subsystems exhibit distributed resistance, compliance, and inertial effects and linear approximations are used for the pulsatile pressure wave flow of blood. The fourth model classification is the nonlinear distributed model which attempts to provide complete pressure and velocity flow descriptions throughout the distributed, time varying circulatory system.

Table 1 shows a brief list of the historical origins and uses of the four levels of modeling.

Concept	**Introduction as a research model**	**Use**
(1)Pure resistance	Young(1809); Poiseuille(1840)	Slow variations of mean blood pressure. Elasticity of microcirculation. Rheology of blood.
(2)Lumped parameter model (windkessel)	Otto Frank (1899)	Stroke volume from aortic pressure. Analog models. Analysis of cardiac assist devices.
(3) Distributed, linear model (transmission line)	Womersley(1957); McDonald(1960)	Computation of flow from pressure gradient. Space and time distribution of pressure and flow. Input impedance studies.
(4)Distributed, non-linear model	Euler(1755); Lambert(1958)	Accurate pressure and flow wave forms.

Table (1) brief list of historical origins and uses of the four levels of modeling [22]

CHAPTER 3

LITERATURE REVIEW

3.1 Introduction

There have been many attempts to model the cardiovascular system in part and as a whole. William Harvey (1578-1657), also known as the 'Father of Hemodynamics', proved that the heart, and not the liver, was the center of the vascular system. His simple compartmental model obeyed the law of mass conservation. He applied Starling's law which states that the external stroke work done by the heart is proportional to end-diastolic ventricular volume within physiological limits. In other words the cardiac output should always be in balance with venous return. This shows that the heart is a self-innervating auto-regulative system. The first mathematical description of blood circulation was attempted by the brilliant mathematician Leonard Euler in 1775. He established a mathematical model for blood circulation, which described viscous, incompressible fluid flow in elastic arteries. Stephen Hales (1677-1761), who is often referred to as a brilliant experimentalist, was the first man to measure arterial blood pressure in the horse. Hales was also the first to compute cardiac output. The first cardiovascular model, more commonly known as the Windkessel model, was designed and developed by Frank Otto in 1899. This very popular model conceives the arteries as a system of interconnected tubes with fluid storage capacity. In an intermittent fashion, commonly known as ventricular ejection, fluid is pumped in at one end, while at the other end through peripheral resistance, outflow is approximately constant and Poiseuillean. On the following page is a representation of the Windkessel model.

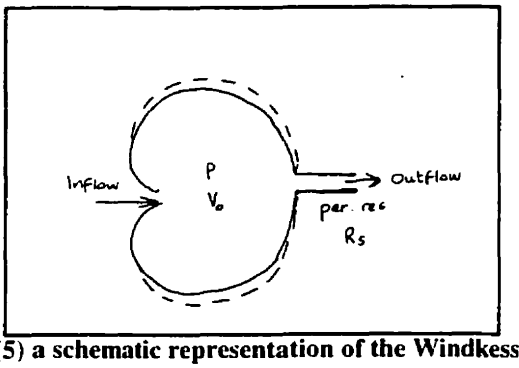

Figure (5) a schematic representation of the Windkessel model

3.2 Brief historical background

This review illustrates some of the more important developments which have been made in relation to physical aspects of the heart and circulation.

3.2.1 Models of Auto-controlled cardiovascular system:

These models describe the instantaneous steady state behaviour of the cardiovascular system. In other words, the heart and circulation form a stable system independent of any other form of control (e.g neural or hormonal).

- Van Harreveld (1949) model used a resistive capacitive electrical analogue. The mean pressures and flows at the outlet and inlet of the heart, as well as the changes when the system parameters varied, were represented. He described the resistance to blood flow by the resistance in the electrical circuit, the capacity for blood storage by charge capacity and blood pressure by voltage. Similar to all the other work done in this period, his model represented the steady state behaviour of the cardiovascular system without taking into consideration the effect of neural or hormonal control.
- Guyton (1955) used a graphical method for the determination of venous return (VR), cardiac output (CO) and arterial pressure (Pa). Guyton plotted CO and VR v/s right atrial pressure (Pra) and the interaction of the two curves determines the operating

point (i.e. when VR=CO), thereby obeying Starling's law. His model also describes the steady state conditions that the system might achieve given limited environmental disturbances.

- Grodins' (1959) resistive capacitive model was based on Starling's law of the heart in which cardiac activity is represented by a linear relationship between stroke work and end-diastolic ventricular volume. The model consists of 23 simultaneous equations, solved to determine the equilibrium values.
- Noordergraaf (1963) used an electrical analogue for the study of human hemodynamics. He devised a mathematical model of the systemic arterial tree (115 segments) to find a quantitative interpretation of the amount of blood passing through the heart in a specific time. This was done by recording the recoil movements of the body that result from contraction of the heart muscle in ejecting blood from ventricles. The blood flow through the left ventricle was assumed to be linear in this model.
- Dick and RideOut (1965) devised a compartmental model which has 4 segments representing the major divisions of the arterial tree and in which pumping of the heart is represented by a time-varying compliance of the left ventricle compartment.
- Beneken (1965) devised a compartmental model similar to that of Dick and RideOut, but with 8 segments and implemented on an analogue computer. The ventricle consists of 2 parts, one concerned with shape and the other with the properties of the wall material. The left ventricle cross-section is assumed to have a cylindrical shape and a constant length. This model, simulated on an electronic analogue, solves 57 equations. Beneken studied the effect of perturbing the parameters on the behaviour of the system as a whole.

- Sandquist, Olsen and Kolff (1982) proposed a comprehensive mathematical model for the mammalian circulatory system based on a set of simplifying assumptions and statements for the hydrodynamic and thermodynamic processes. Their aim was to provide a correct quantitative description of the behavior and interaction of blood flow through the major subsystems and compartments of the circulatory systems.
- Burkhoff et al. (1993) developed a mathematical model to simulate the cardiovascular system. The ventricles are represented by time-varying elastances. The systemic and pulmonary circuits are each modeled as lumped venous and arterial capacitances, a proximal characteristic resistance, and lumped venous and arterial resistances. This model will be further described in section 3.6.

3.2.2 Models of Controlled Cardiovascular Systems:

(I) Pulsatile models

- Warner (1959) included pulsatile phenomena in his resistive-inductive capacitive model of the closed circulatory system. He set the structural pattern for subsequent studies. His system was subdivided into a number of sections with the condition that outflow of any segment is the same as the inflow of the next segment.
- Beneken and De Wit (1967) constructed compartmental model consisting of 19 segments representing the heart chambers, major arterial and venous vessels. The specific shapes of the ventricles and properties of the ventricular wall are also taken into consideration. This model is described in more detail in section 3.3.
- Beneken and RideOut (1968) showed that computer models of the circulation based on lumped circuit approximations may be used for simulation studies of its pulsatile pressure, flow and volume relationships. Coupled to this basic circulation model, a

second model may be developed to simulate the flow of substances carried by the blood. Such a dependent model is based on the notion that transport flow is proportional to concentration in the dependent circuit multiplied by flow in the main circuit. The combined model can be used to control studies related to the transport of carbon-dioxide and oxygen.

- Pullen (1976) based his model structure on the circulatory fluid mechanics of Beneken and De Wit (1967) with baroreceptor and neural control models of Katona (1967) and Hyndman (1970) and the "multiple modeling" of Beneken and RideOut (1968). Pullen introduced an algebraic method for modeling the local effects of cardiovascular active drugs.
- Piene (1983) developed a 7-segment model based on Beneken (1964) model. His model consisted of 4 active heart chambers, 1 pulmonary bed, 1 systemic arterial bed and 1 venous bed. The heart chambers are contained in an elastic pericardium whose P-V (pressure volume) relationship was linear. This model is further described in section 3.5.

(II) Non-pulsatile models

- Boyers (1972) developed a non-pulsatile control model of the cardiovascular system to study normal responses to posture, blood loss, transfusion and autonomic blockade. The model consists of the heart, large arteries, peripheral circulation and the effects of a ganglionic agent (Arfonad) on the circulatory response to a large transfusion of blood. The model simulates the steady state responses of the cardiovascular system to stresses ranging from a few seconds to many hours in duration. It can also be used to study the regulation of interstitial fluid and total blood volumes. The results obtained

from the tests of the model agree closely with measurements made on the human circulation.

- Guyton et al. (1972) devised a non- pulsatile lumped-parameter model of the uncontrolled circulation to which was added a large number of short and long term control mechanisms. The analysis consisted of 354 blocks, each of which represents at least one mathematical equation describing some physiological facet of circulatory function. Guyton divided the analysis into 18 different major systems that enter into circulatory control. The model contains the blood conductive pathway, vascular stress, relaxation, membrane dynamics of the capillaries, tissue fluid volume and pressure, electrolyte shift, autoregulation, autonomic control amongst a number of other facets. This led to an equation set of order 37 which was solved using a digital computer.
- Leaning et al. (1983) reported a model originally devised by Pullen, based on the Beneken and De Wit (1967) model of 19 compartments. The objective here was to study hemodynamic and drug effects in the CNS controlled cardiovascular system. This model is described in more detail in section 3.4.

3.3 Overview of Beneken and De Wit model

Figure (6) shows a block diagram of the cardiovascular system with its subdivision into 19 segments; seven systemic arterial segments, six systemic venous segments, four heart chambers and two pulmonary segments. Two arterial and two venous segments represent the intra-abdominal vessels, while three arterial and two venous segments of the systemic circulation represent the intra-thoracic vessels. This compartmental model takes into account the specific shapes of the ventricles and properties of the ventricular wall. The

contractile properties of the heart muscle are included by equations relating length, force, velocity, and time based on physiological data. The contractile actions of the atria are incorporated as time-varying elastances. The description of the systemic and pulmonary vascular systems covers elastic and viscous wall properties, inertia and viscosity of blood, proper distribution of blood volume between the various compartments and cardiac output in the lumped arterio-venous pathways. An electrical analogue computer was used to solve the simultaneous equations. The simultaneous solution of all equations involved raises the possibility of studying the behaviour of the system as a whole and of investigating its sensitivity to parameter variations.

The equations governing this model are as follows. The relation between volume inflow and outflow (equation of continuity) is

$$V_{LV}(t) = V_{OLV} + \int (F_{LALV} - F_{LVAOI})dt \tag{3.1}$$

The equation of motion is the relation between the left ventricular pressure P_{LV}, the pressure in the ascending aorta, and left ventricular outflow. The equation is similar for the right ventricles, thus

$$P_{LV} - P_{AOI} = R_{LVAOI}F_{LVAOI} + L_{LV}\frac{dF_{LVAOI}}{dt} + \frac{\rho}{2A^2_{AOI}}F^2_{LVAOI} \tag{3.2}$$
$$F_{LVAOI} = 0 \text{.....} if \text{.....} P_{LV} \le P_{AOI}$$

The atria are modeled as time-varying elastances, thus;

$$P_{LA} = a_{LA}(t)(V - V_u)_{LA}$$
$$P_{RA} = a_{RA}(t)(V - V_u)_{RA} \tag{3.3}$$

The pulmonary and systemic vessels are modeled by the following equations:

$$P_0 - P_1 = R_1 F_{01} + L_1 \frac{dF_{01}}{dt} \tag{3.4}$$

$$V_1 = V_{01} + \int (F_{01} - F_{12}) dt \tag{3.5}$$

$$P_1 = \frac{1}{C_1}(V - V_u)_1 + R_1' \frac{dV_1}{dt} \tag{3.6}$$

where C is compliance, L is inertance, F is flow (here in first segment), V is volume, R is resistance, R' is viscosity coefficient and V_u is unstressed volume.

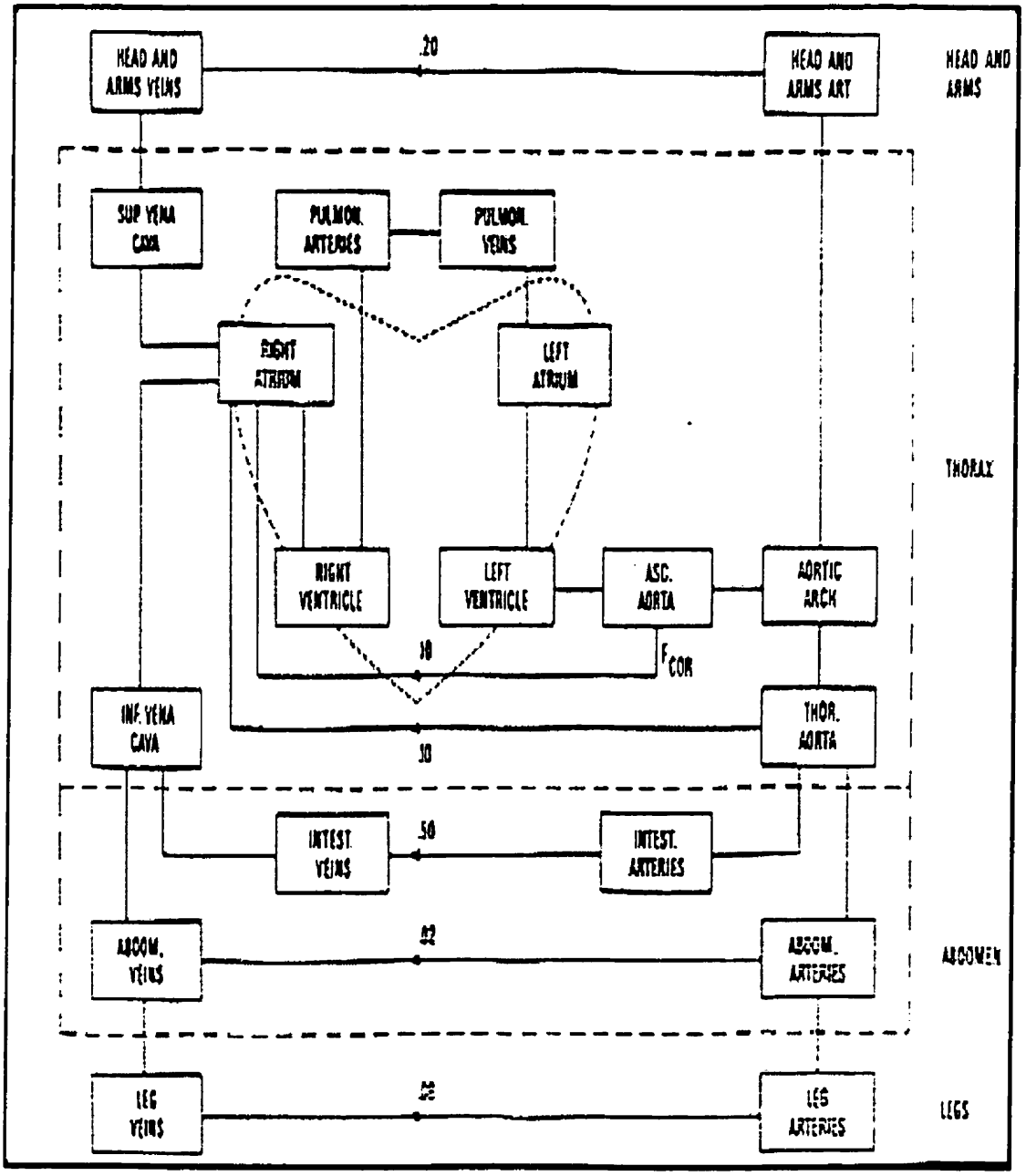

Figure (6) block diagram of the cardiovascular system. [32]

3.4 Overview of Leaning et al. model

Leaning et al. (1983) based his model on the Beneken and De Wit (1967) model of 19 compartments. The objective here was to study hemodynamic and drug effects in the

CNS controlled cardiovascular system. The model consists of 61 state equations and 178 parameters in total. Leaning et al. carried out tests based on a comprehensive and systemic program of validation of the circulatory, neural control and local pharmacodynamic subsystems of the model. Emphasis was put on validation aspects of modeling methodology. Many validation problems occurred because of the large size of the model. The limitations and the possibilities of model reduction and development were considered.

Below is a list of the equations used in the model.

Equations of the fluid mechanics subsystem:

For all segments j, from continuity considerations:

$$\frac{dV_j}{dt} = \sum_i F_{ij} - \sum_k F_{jk} \quad V_j \geq 0, \quad \text{for all } j \tag{3.7}$$

Arterial segments

$$\frac{dF_{jk}}{dt} = \frac{(P_j - P_k - \sigma_{jk} R_{jk} F_{jk} - G_{jk})}{L_k}$$

where

$$G_{jk} = ngl_{jk} \sin\phi_{jk} \tag{3.8}$$

$$P_j = \frac{1}{c_j}(V_j - V_{uj}) + \frac{K_j}{c_j}\frac{dV_j}{dt}$$

Heart Segments, *j*:

$$P_j = a_j(t)(V_j - V_{uj}) \tag{3.9}$$

For ventricle segments:

$$\frac{dF_{jk}}{dt} = \frac{[P_j - P_k - R_{jk} F_{jk} + F_{jk}^2(\rho / 2A_j^2)]}{L_j} \qquad F_{jk} \geq 0 \tag{3.10}$$

$$a_j(t) = y(b_2\sigma_j a_{jS} - a_{jD}) + a_{jD} \tag{3.11}$$

For atrial segments

$$F_{jk} = \frac{(P_j - P_k)}{R_{jk}} \qquad F_{jk} \geq 0 \tag{3.12}$$

$$a_j(t) = y(b_2\sigma_j a_{jS} - a_{jD}) + a_{jD}$$

Timings of the cardiac cycle

The heart is considered as a set of four separate unidirectional pumps. Cardiac timing events are similar to those used in the Beneken and De Wit model.

$$T_{AS} = 0.1 + 0.09\, T_H$$

$$T_{AV} = T_{AS} - 0.04 \tag{3.13}$$

$$T_{VS} = 0.16 + 0.2 T_H$$

where T_{AS} is the period of arterial systole, T_{AV} is the time between the start of arterial systole and the start of ventricular systole, T_{VS} is the period of ventricular systole, and T_H is the heart period.

$$x = 0 \qquad , t_c > T_{AS}$$
$$x = \sin(pi * t_c / T_{AS}) \qquad , t_c < T_{AS}$$

$$y = 0 \qquad , t_c < T_{AS} \text{ or } t_2 > T_{AV} + T_{VS} \tag{3.14}$$
$$y = \sin(pi * (t_c - T_{AV}) / T_{VS}) \qquad , T_{AV} < t_2 < T_{AV} + T_{VS}$$

For all venous segments

$$P_j = \frac{1}{c_j}(V_j - V_{uj}) \qquad \text{where } c_j = c_{uj}, \quad Vj > Vuj \tag{3.15}$$

$$c_j = \alpha_j c_{uj}, \quad Vj \leq Vuj$$

$$F_{jk} = (P_j - P_k) V_j^2 \qquad Pj < Pk \tag{3.16}$$

$$F_{jk} = \frac{\beta_j (P_j - P_k) V_j^2}{R_{jk} V_{uj}^2} \qquad Pj < Pk \tag{3.17}$$

3.5 Overview of Piene et al. model

The model of Piene et al. [28] resembled that proposed by Beneken in 1964. It consisted of 4 active heart chambers (atria and ventricles) which were modeled by time-varying compliances. The atria and ventricles were connected to each other by unidirectional valves and small resistances. The right ventricle was connected to the left atria by a lumped windkessel model of the pulmonary circulation. The left ventricle was connected to the venous system through a similar representation of the systemic arteries. The venous bed was represented by a large compliance and a small inflow resistance to the right atrium. The four heart chambers were contained within an elastic pericardium.

The time varying systolic ventricular elastance:

$$E_v(t) = C\,E_{max}\,sin\,(2\pi(2t-0.25)) \qquad (3.18)$$

where C =contractility, and E_{max} is the maximum systolic elastance.

The time-varying systolic atrial elastance:

$$E(t) = 6E_d\,(sin\,(2\pi(2t-0.05)-0.75) \qquad (3.19)$$

where E_d is the diastolic atrial elastances.

The aim of this work was to examine the potency of a simple model of the circulatory system for the interpretation of experimentally obtained data. Piene et al. proved that alteration of myocardial function of a compartment of the intact heart will influence the other compartments. The pressure-volume relationship of a specific heart compartment is depicted by the myocardial stiffness plus the effects of pericardial constraint. It was also

shown that, owing to the fact that the heart chambers are arranged in series, the end-diastolic dimensions have to adjust until the outputs on both sides of the heart balance. Below is a schematic representation of the model used by Piene et al.

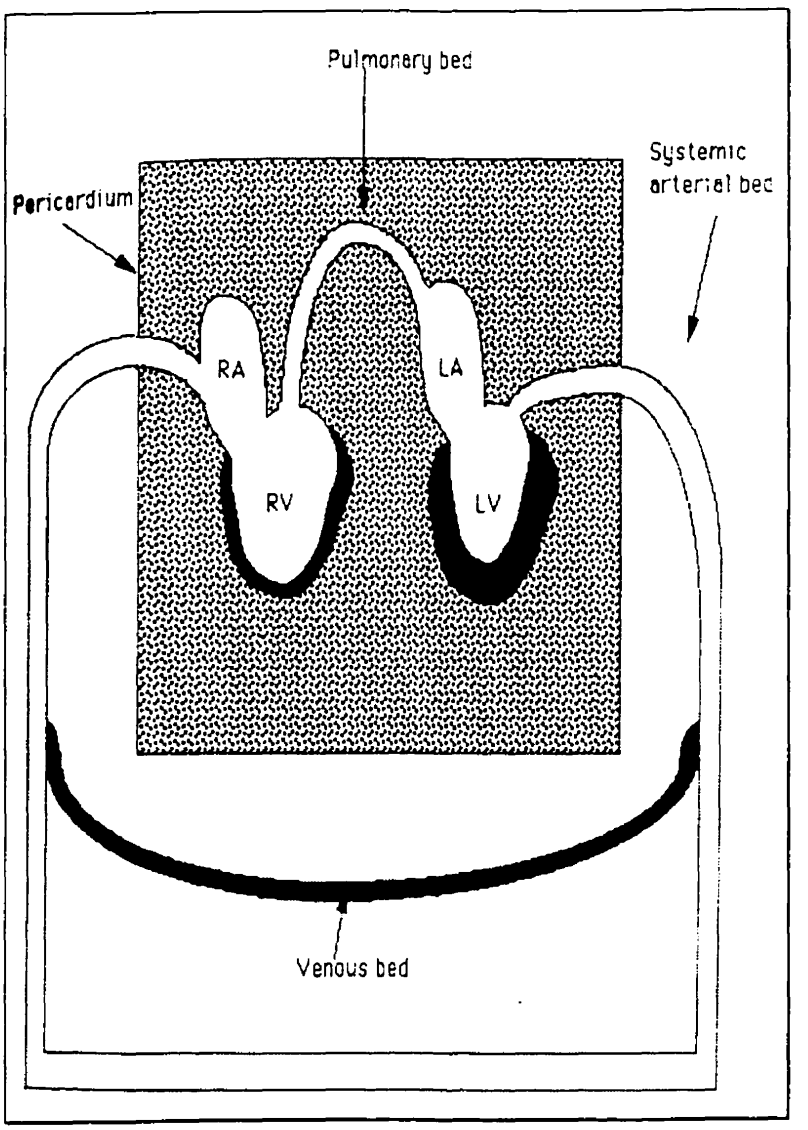

Figure (7): sketch of Piene et al. model (1983).[36]

3.6 Overview of Burkhoff and Tyberg model

The question addressed by Burkhoff and Tyberg [7] in 1993 study was "Why does pulmonary venous pressure rise after onset of LV dysfunction". The aim of their analysis was thus to assess the relative importance of decreased ventricular contractile state, increased heart rate, increased arterial resistance, and decreased venous capacity in the development of pulmonary congestion after the onset of LVD (left ventricular dysfunction).

Figure (8) shows a representation of the modeled cardiovascular system:

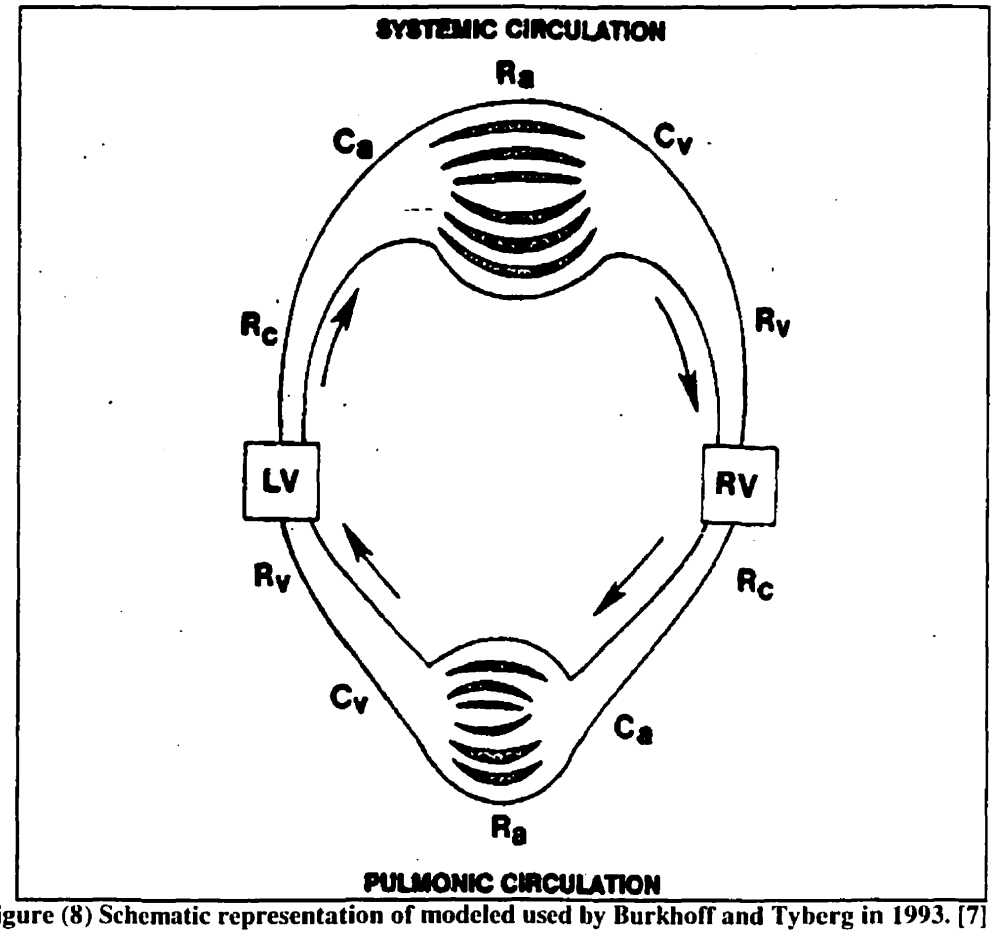

Figure (8) Schematic representation of modeled used by Burkhoff and Tyberg in 1993. [7]

Both the systemic and pulmonary circuits are the modeled by lumped venous and arterial capacitances, a proximal characteristic resistance, a lumped arterial resistance and a

resistance to return blood from the veins to the heart. The right and left ventricular pumping actions are given by time-varying elastances, which relate instantaneous ventricular pressure linearly to instantaneous volume. The model assumes a non-linear end-diastolic pressure-volume relationship, a linear end-systolic pressure-volume relationship, and a smooth progression between the two during the cardiac cycle.

End-diastolic pressure (P_{ed}) and volume (V_{ed}) are related by

$$P_{ed}=A\,[e^{B(Ved-V_0)}-1] \tag{3.20}$$

where A and B are constants. End –systolic pressure (P_{es}) and volume (V_{es}) are related by

$$P_{es} = E_{es}\,(V_{es}-V_0) \tag{3.21}$$

where E_{es} is the maximal volume elastance, V_0 is the volume at which end-systolic pressure is 0mmHg. A function $e\,(t)$ depicts the time-course of the chamber stiffness between end-systole and end-diastole, thus;

$$e\,(t)=0.5[\sin\,(\pi t/T_{es}-\pi/2)+1\,] \qquad for\ \ t < 3T_{es}/2$$

$$e\,(t)=0.5\,e^{[(t-3Tes/2)/\tau]} \qquad for\ \ t > 3T_{es}/2 \tag{3.22}$$

where T_{es} is the time for end-systole and τ is the time constant of relaxation.

A set of six differential equations describes changes in volumes of the four vascular compartments and the two ventricles as functions of time. These simultaneous differential equations were solved numerically.

CHAPTER 4

MODEL DEVELOPMENT

4.1 Mathematical description of Model subsystems

4.1.1 Model

A schematic representation of the cardiovascular system is shown in Figure (9). The model is based on that of Burkhoff and Tyberg model [7] and consists of 6 lumped compartments; the left heart, systemic artery, systemic vein, pulmonary artery, pulmonary vein, and right heart. The reasons why this project was based on the model by Burkhoff and Tyberg [7] are:

(1) Burkhoff and Tyberg's model had a very useful approach to analysis using lumped compartments.

(2) Burkhoff and Tyberg's model closely matched the layout of the cardiovascular circulation.

(3) Their model was the latest and most up to date model of the four models that have been presented in this project.

(4) Dr. S. Magder and I were interested in re-investigating the particular application performed by Burkhoff and Tyberg [7].

The modifications to this model investigated in the first part of the present project are:

(1) the ratio of venous systemic resistance (Rvs) to venous pulmonary resistance (Rvp) was changed from 1:1 to 1:6.

(2) the ratio of the venous systemic compliance (Cvs) to the arterial systemic compliance (Cas) was changed from 1:70 to 1:30.

(3) the ratio of total pulmonary compliance (Cvs + Cvp) to total systemic compliance (Cas +Cap) was changed from 1:3 to 1:7.

(4) the stressed volume (Vs) was raised from 750ml to 1830ml.

These ratios of Rvs: Rvp, Cvs: Cas, (Cvs+Cvp): (Cas+Cap) that were chosen for this project are reflective of the ratios obtained from Dr. Magder's experimental data. Furthermore the ratios used in this project are supported by data presented in the literature [12, 13, 14]. The model simulates a normal 70kg man in whom the Cardiac Output (CO) ~= 5 l/min, the MAP ~= 90mmHg, Pvs ~= 6-8 mmHg, and PVP ~= 8-12mmHg.

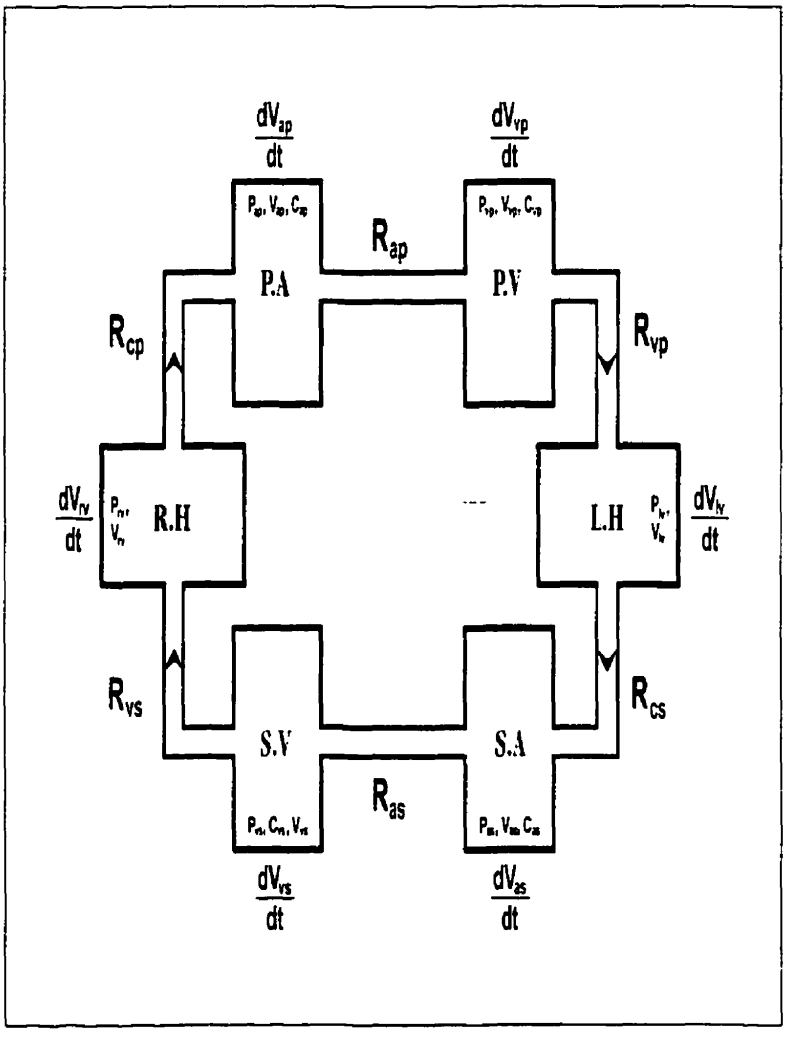

Figure (9) Structure of the Model used in the present study

4.1.2 Model structure and equations

Blood flow through the circulatory system is described by a set of simultaneous linear differential equations. The general equations illustrating a typical segment are derived considering two typical segments, which are connected as shown below.

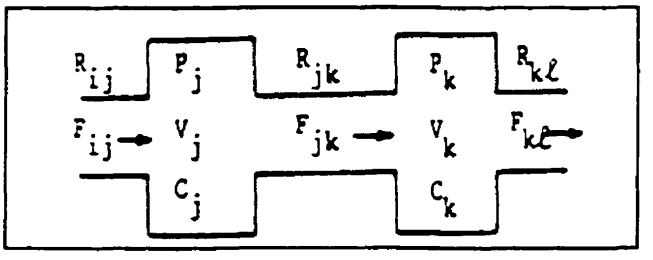

Figure (10): Two typical adjoining lumped parameter segments

The systemic and pulmonary circuits are modeled as lumped venous and arterial capacitances, a proximal characteristic resistance relating the stiffness of the proximal aorta or pulmonary artery, a lumped arterial resistance, and a resistance to return of blood from the lumped venous to the heart. The heart valves allow flow in only one direction through the circuit.

Below are the differential equations describing changes in volumes in the five capacitors and the two ventricles as functions of time in terms of the pressure across each compartment and the resistance between them. Refer to Appendix 2 for a list of the subscripts, symbols and units employed.

Model

$$\frac{dV_{as}(t)}{dt} = \frac{P_{lv}(t) - P_{as}(t)}{R_{cs}}\beta_{lv} - \frac{P_{as}(t) - P_{vs}(t)}{R_{as}} \tag{4.1}$$

$$\frac{dV_{vs}(t)}{dt} = \frac{P_{as}(t) - P_{vs}(t)}{R_{as}} - \frac{P_{vs}(t) - P_{rv}(t)}{R_{vs}}\alpha_{rv} \tag{4.2}$$

$$\frac{dV_{rv}(t)}{dt} = \frac{P_{vs}(t) - P_{rv}(t)}{R_{vs}}\alpha_{rv} - \frac{P_{rv}(t) - P_{ap}(t)}{R_{cp}}\beta_{rv}. \tag{4.3}$$

$$\frac{dV_{ap}(t)}{dt} = \frac{P_{rv}(t) - P_{ap}(t)}{R_{cp}}\beta_{rv} - \frac{P_{ap}(t) - P_{vp}(t)}{R_{ap}} \tag{4.4}$$

$$\frac{dV_{vp}(t)}{dt} = \frac{P_{ap}(t) - P_{vp}(t)}{R_{ap}} - \frac{P_{vp}(t) - P_{lv}(t)}{R_{vp}}\alpha_{lv} \tag{4.5}$$

$$\frac{dV_{lv}(t)}{dt} = \frac{P_{vp}(t) - P_{lv}(t)}{R_{vp}}\alpha_{lv} - \frac{P_{lv}(t) - P_{as}(t)}{R_{cs}}\beta_{lv} \tag{4.6}$$

$$P_{as} = \frac{V_{as}}{C_{as}} \tag{4.7}$$

$$P_{vs} = \frac{V_{vs}}{C_{vs}} \tag{4.8}$$

$$P_{ap} = \frac{V_{ap}}{C_{ap}} \tag{4.9}$$

$$P_{vp} = \frac{V_{vp}}{C_{vp}} \tag{4.10}$$

4.1.3 Model of the heart

The right and left ventricular pumping characteristics are represented by time-varying elastance theory relating instantaneous ventricular pressure linearly to instantaneous volume:

$$P(t)=E(t)[V(t)-Vo] \tag{4.11}$$

$E(t)$ is modeled as a raised sine wave during systole and an exponential decay during diastole (Figure (11)). This model assumes a nonlinear end-diastolic pressure-volume relationship, a linear end-systolic pressure-volume relationship, and a smooth progression between the two during the cardiac cycle.

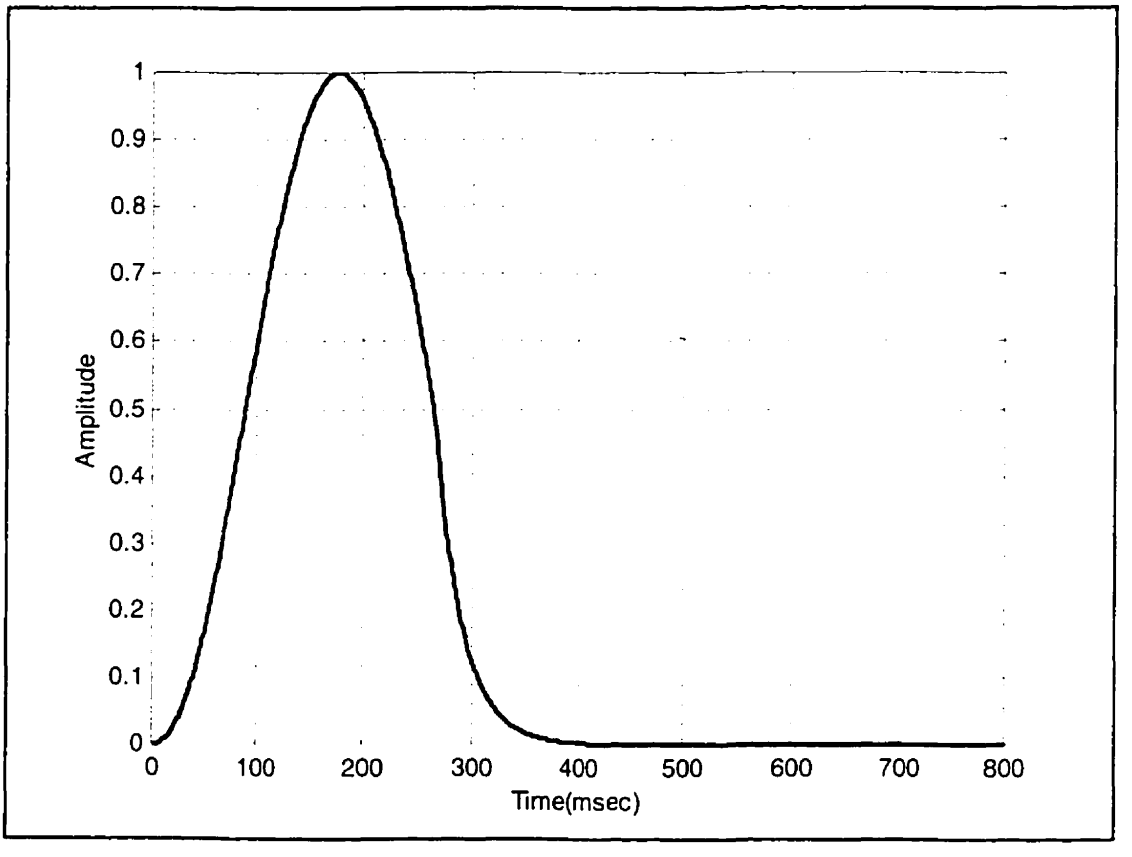

Figure 11: Representation of E (t) function

$$P_{lv}(t) = [P_{eslv}(V_{lv}) - P_{edlv}(V_{lv})]\varepsilon_{lv}(t) + P_{edlv}(V_{lv}) \tag{4.12}$$

where

$$\varepsilon_{lv}(t) = \frac{1}{2}[\sin(\frac{\pi}{T_{es}}t - \frac{\pi}{2}) + 1] \tag{4.13}$$

$$for\_t < \frac{3T_{es}}{2}$$

$$\varepsilon_{lv}(t) = \frac{1}{2}\exp[\frac{(t - (3T_{es}/2)}{\tau}] \tag{4.14}$$

$$for\_t \geq \frac{3T_{es}}{2} \tag{4.15}$$

$$P_{eslv}(V_{lv}) = E_{eslv}(V_{lv} - V_{olv})$$

$$P_{edlv}(V_{lv}) = A_{lv}\{\exp[B_{lv}(V_{lv} - V_{olv})] - 1\}) \tag{4.16}$$

A set of equations similar to the one above is used to describe the right heart. The volume of blood in each compartment is divided into two pools denoted the unstressed and the stressed volumes. Unstressed volume is the maximum volume that can be placed in a capacitive vessel without raising its pressure above 0 mmHg. The pressure within the compartment is assumed to increase linearly with stressed volume. The total stressed volume of the body equals the sum of the stressed volume of all compartments.

Therefore, total volume in the body is broken down as follows:

$$V_T = V_{as} + V_{ap} + V_{vs} + V_{vp} + V_{lv} + V_{rv} + V_u \tag{4.17}$$

4.1.4 Pericardial Effect

The right and left heart properties are interdependent, since they share a common wall known as the septum and they are encased in a sac called the pericardium. The effect of the pericardium is incorporated into the model by adjusting the function of the right heart, through the end-diastolic right ventricular pressure-volume curve. The original relationship used by Burkhoff and Tyberg was modified to be:

$$Pedrv = Crv \times [Arv \times (exp\ (Brv \times (Vrv - Vorv)) - 1] \quad (4.18)$$

$$Pesrv = Eesrv \times (Vrv - Vorv) \quad (4.19)$$

where Crv =0.05, Arv=0.002, and Brv=0.098

The new Pressure-Volume Relationship of the End-diastolic curve is given in Figure (12).

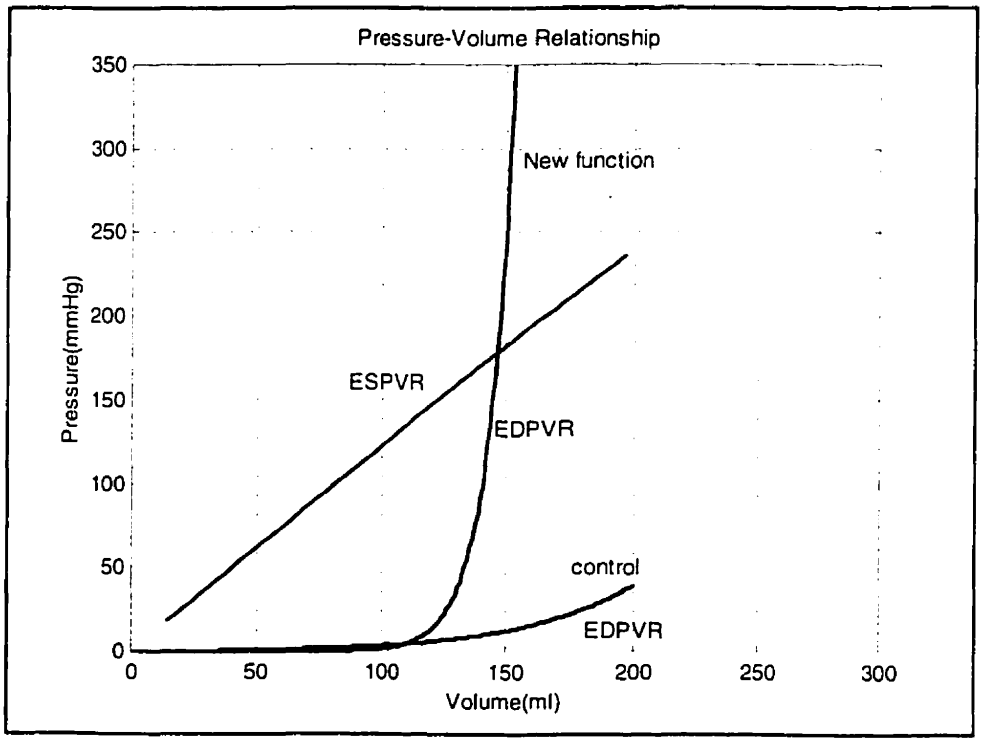

Figure (12) Representation of pressure-volume relationship for end-diastolic curve.

4.2 Implementation

4.2.1 Simulink

Simulink is a software package, built on top of MATLAB®*, for modeling, simulating, and analyzing dynamical systems. It supports linear and nonlinear systems and model in continuous time or sampled time or a hybrid of the two. Also, systems can be multi-rate, that is, have different parts that are sampled or updated at different rates.

Simulink provides a graphical user interface for building models as block diagrams, using click-and-drag mouse operations. It includes a comprehensive block library of sinks, sources, linear and nonlinear components, and connectors. It also allows customization of existing blocks and creation of new ones.

Models are hierarchical, and can be built using either top-down or bottom-up approaches. They can be viewed at a variety of levels of detail. This provides insight into how the various parts of the model interact.

Once a model has been defined, simulation is performed, using a choice of integration methods, either from the Simulink menus or by entering commands in MATLAB's command window. The menus are especially useful for interactive work, while the command-line approach is very convenient for running a batch of simulations. With the use of scopes and other display blocks, the simulation results can be viewed while the

* MATLAB is owned by The MathWorks, Inc. 3 Apple Hill Drive Natick, MA 01760-2098 UNITED STATES; http://www.mathworks.com

simulation is running. Also, parameters can be changed during simulation. The simulation results can be forwarded to the MATLAB workspace for post-processing and visualization.

The solver used for this model was ode* 5 (Dormand –Prince) with a fixed step size of 0.001 and a single-tasking mode. The time period for one simulation was set to 72 seconds.

A Simulink representation of the model used in the preset study is given in Figure (13). The Simulink representation model of the heart is given on Figure (14).

---

* ode = ordinary differential equation

Figure (13) Representation of model in Simulink

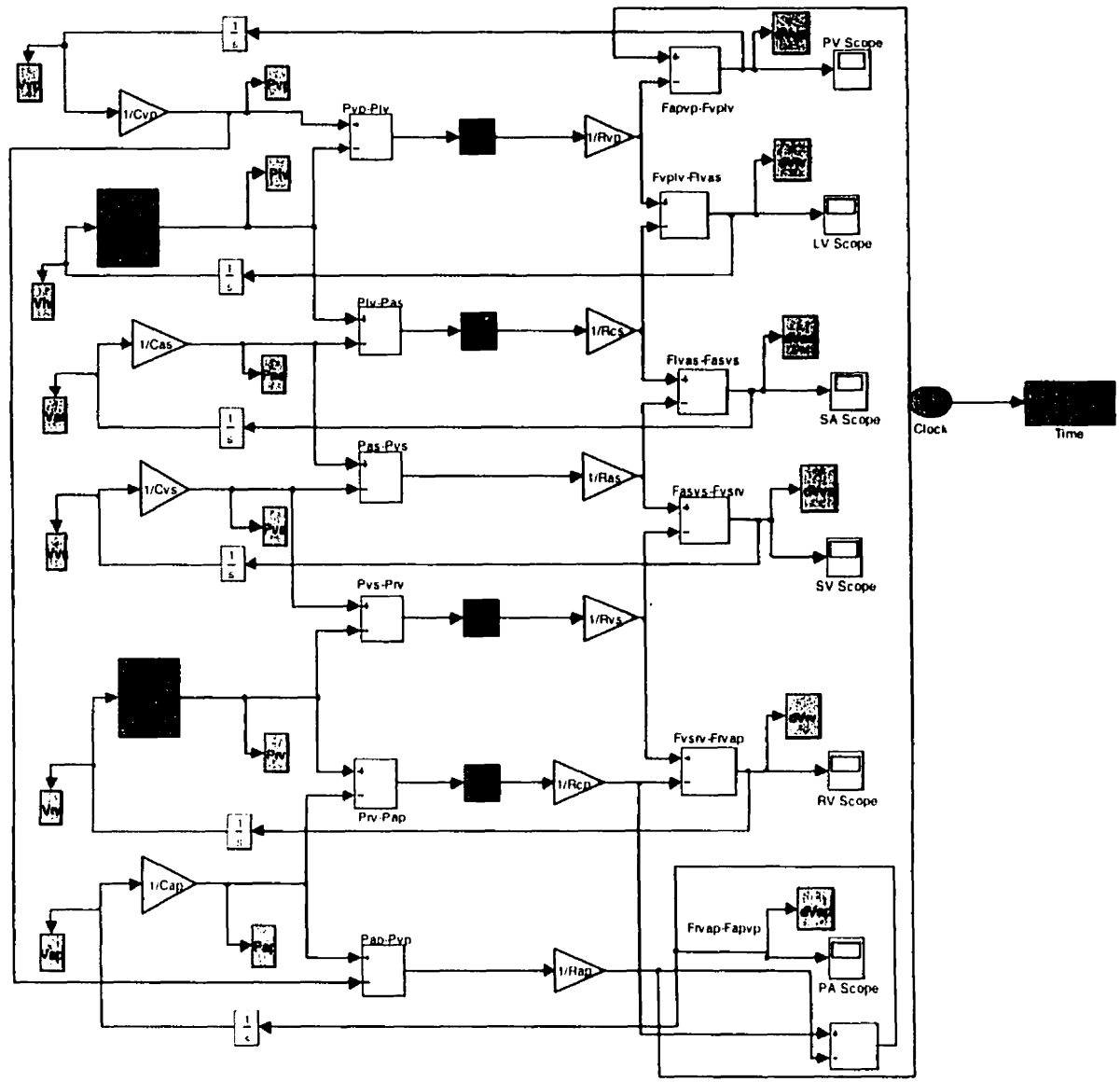

Figure (14) Simulink representation of left and right heart

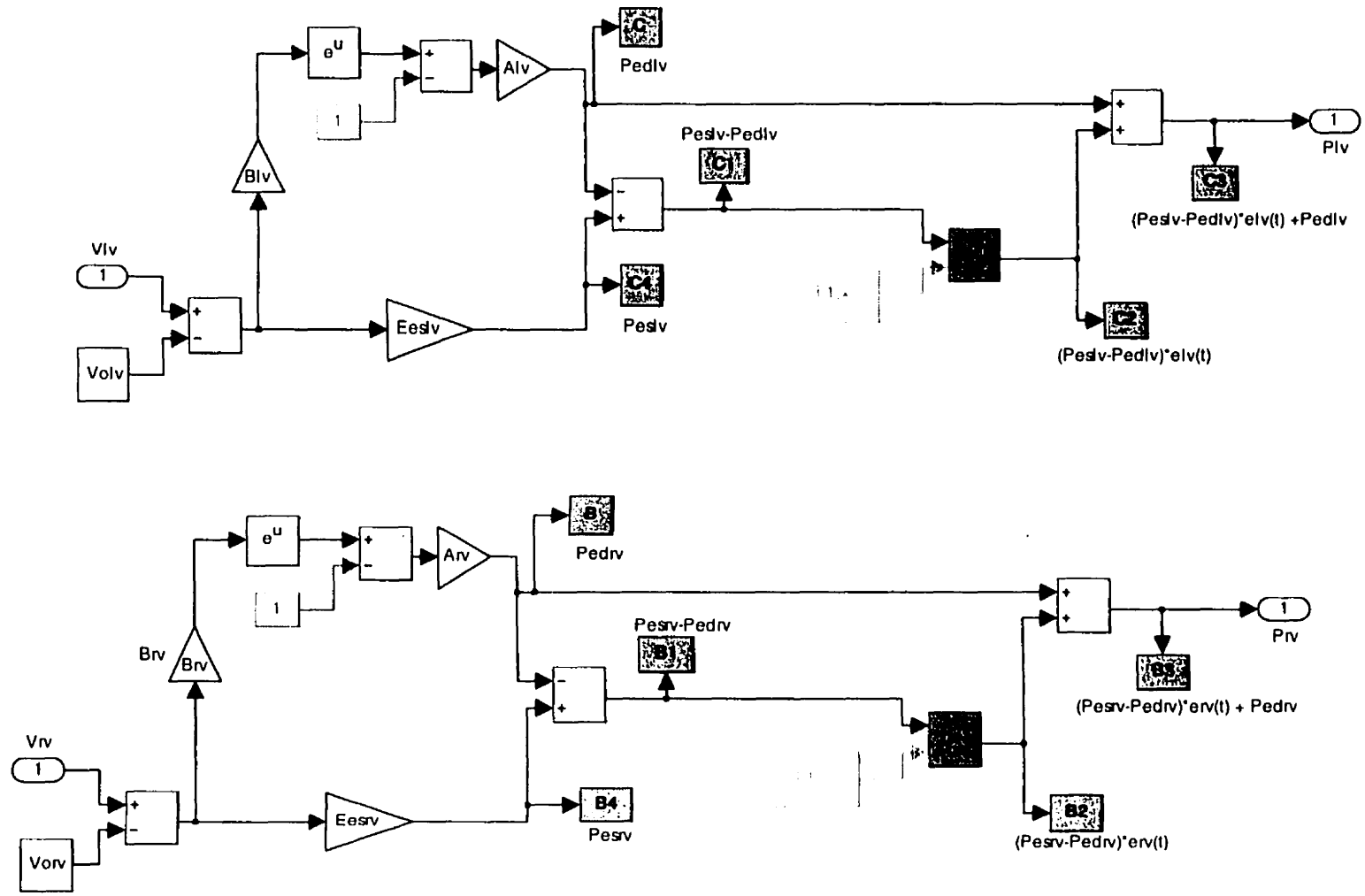

CHAPTER 5

SIMULATIONS AND APPLICATIONS

5.1 Control parameter values

Model

Heart parameters	**Right Ventricle**	**Left Ventricle**
Ees (end-systolic elastance) (mmHg/ml)	Eesrv = 1.2	Eeslv = 4
Unstressed volume (Vo) (ml)	Vorv = 0	Volv = 0
Time to end systole (ms)	Tes = 125	Tes = 125
Time constant of relaxation (ms)	τ= 25	τ= 25
Scaling factor for EDPVR (mmHg)	Arv = 0.35	Alv = 0.35
Exponent for EDPVR (mmHg)	Brv = 0.023	Blv = 0.033
Circulation parameters	**Pulmonary**	**Systemic**
Arterial resistance (mmHg.s/ml)	Rap = 0.0312	Ras = 1.0005
Characteristic resistance(mmHg.s/ml)	Rcp = 0.021	Rcs = 0.0312
Venous resistance (mmHg.s/ml)	Rvp = 0.01	Rvs = 0.06
Arterial capacitance (ml/mmHg)	Cap = 6.3	Cas = 4
Venous capacitance (ml/mmHg)	Cvp = 14.7	Cvs = 140
Common parameters		
Heart Rate (beats/min)		HR = 75
Total stressed blood volume (ml)		Vs = 1830

Table (2) parameter values chosen to be appropriate for 70-kg man

	Control values	Range of normal values
EDLV (End diastolic left ventricular vol.)	92.307 ml	-------
EDRV (End diastolic right ventricular vol.)	79.694 ml	-------
ESLV (End systolic left ventricular vol.)	24.978 ml	-------
ESRV (End systolic right ventricular vol.)	12.381 ml	-------
SV (Stroke Volume)	67.313 ml	60-70 ml
CO (cardiac output)	5.048 l/min	4-6 l/min
PVP (Pulmonary venous pressure)	9.644 mmHg	8-15 mmHg
MAP (Mean arterial pressure)	90.013 mmHg	~90 mmHg
PVS (Systemic vein pressure)	8.47 mmHg	~8-10 mmHg
Pedlv(End diastolic left ventricular pressure)	1.838 mmHg	0-2 mmHg
Pedrv (End diastolic right ventricular pressure)	7.012 mmHg	4-6 mmHg
(E.F) ejection fraction	0.729	------

Table (3) showing the control values obtained from control simulation

Table (2) shows the control parameters, as well as their respective symbols and units used in this extended model. Table (3) represents the variables that are calculated from a control simulation of the model and the normal range within which they are supposed to lie for a normal 70-kg man.

5.2 Sensitivity Analysis

A sensitivity analysis of the model was performed by perturbing each of the parameters in turn, by ± 5% and observing the changes in cardiac output (CO), mean arterial pressure (MAP), End-diastolic right ventricular pressure (Pedrv), pulmonary venous pressure (PVP), and systemic venous pressure (PVS). The analysis was performed for both the Burkhoff and Tyberg model and our extended model. Excel was used to chart the results.

The parameter of major concern here is the systemic venous resistance (Rvs). On perturbation within ±5%, major differences are noted when comparing the results obtained by Burkhoff and Tyberg model and our extended model. CO varied within ~±0.1% for Burkhoff and Tyberg and ~±2.2% for our model. MAP varied within ~±0.9% for Burkhoff and Tyberg model and ~±1.8% for our model. PVP varied within ~±0.3% for Burkhoff and Tyberg and ~±5% for our model. Pedrv varied within ~±0.4% for Burkhoff and Tyberg model and ~±5.5% for our model. PVS varied within ~±0.2% for Burkhoff and Tyberg model and ~±2.2% for our model.

These observable differences can be attributed to the fact that our ratio of systemic to pulmonary resistance was 1:6 compared to the 1:1 of Burkhoff and Tyberg. From a physiological basis, on perturbation of the peripheral resistance, one should obtain a larger fluctuation than that obtained by Burkhoff and Tyberg, and similar to our results. Hence our ratios are a better representation of the cardiovascular circulation than those used by Burkhoff and Tyberg [7].

For sake of completeness, the remainder of the parameters was also perturbed and the results charted.

Sensitivity Analysis with Perturbation of (+/-5%)[values are given as percent change]

Burkhoff/ Tyberg model

The plots below are charts representing the percent change in CO, MAP, PVP, PVS, Pedrv, and respectively with +/-5% changes in each parameter in turn.

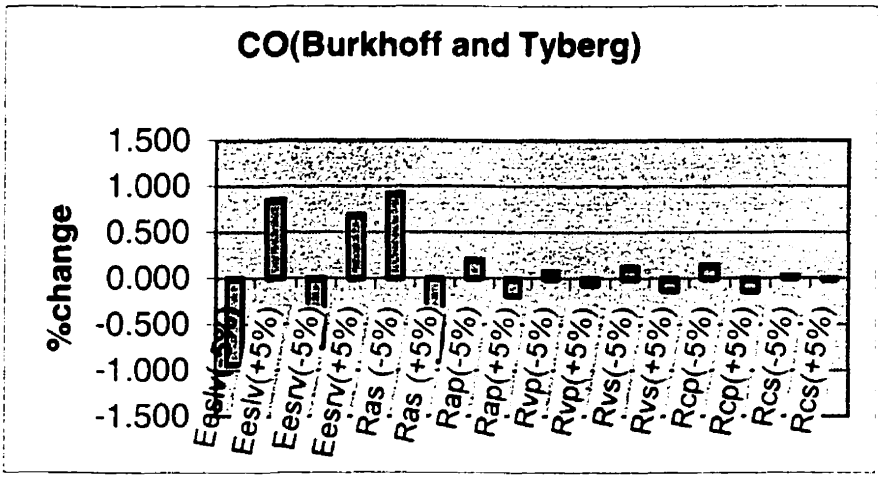

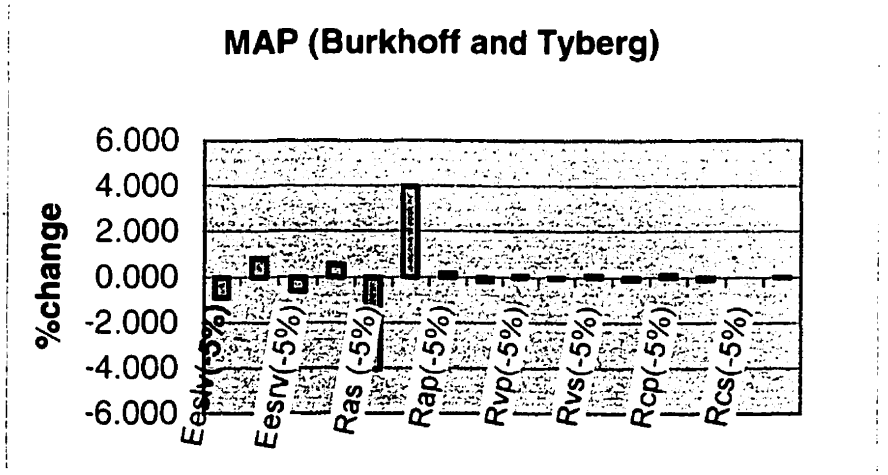

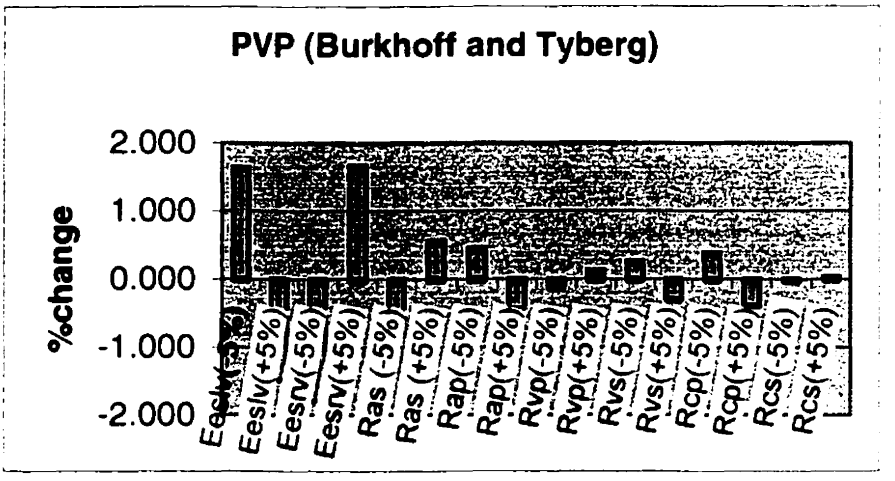
PVP (Burkhoff and Tyberg)
%change
2.000
1.000
0.000
-1.000
-2.000
Eesv(+5%)
Eesv(-5%)
Ras (+5%)
Ras (-5%)
Rap(+5%)
Rap(-5%)
Rvp(+5%)
Rvp(-5%)
Rvs(+5%)
Rvs(-5%)
Rcp(+5%)
Rcp(-5%)
Rcs(+5%)
Rcs(-5%)

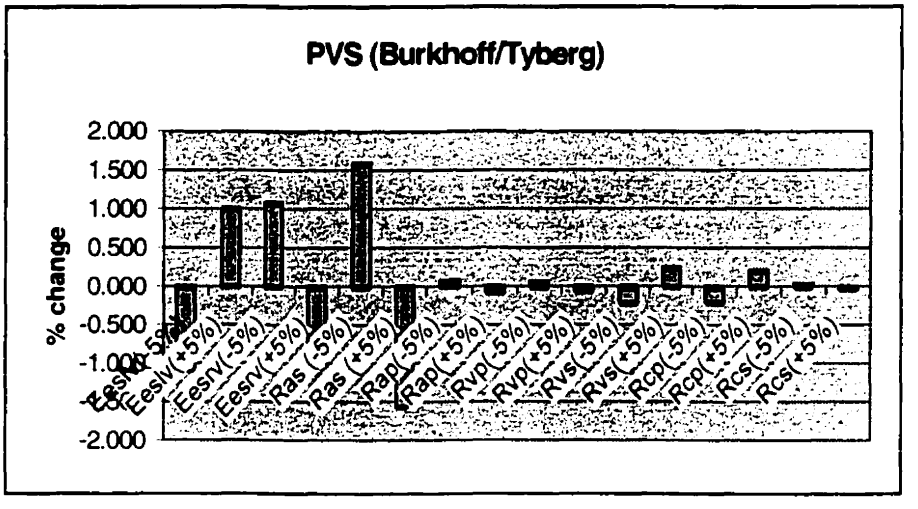
PVS (Burkhoff/Tyberg)
% change
2.000
1.500
1.000
0.500
0.000
-0.500
-1.000
-2.000
Eesv(+5%)
Eesv(-5%)
Ras (+5%)
Ras (-5%)
Rap(+5%)
Rap(-5%)
Rvp(+5%)
Rvp(-5%)
Rvs(+5%)
Rvs(-5%)
Rcp(+5%)
Rcp(-5%)
Rcs(+5%)
Rcs(-5%)

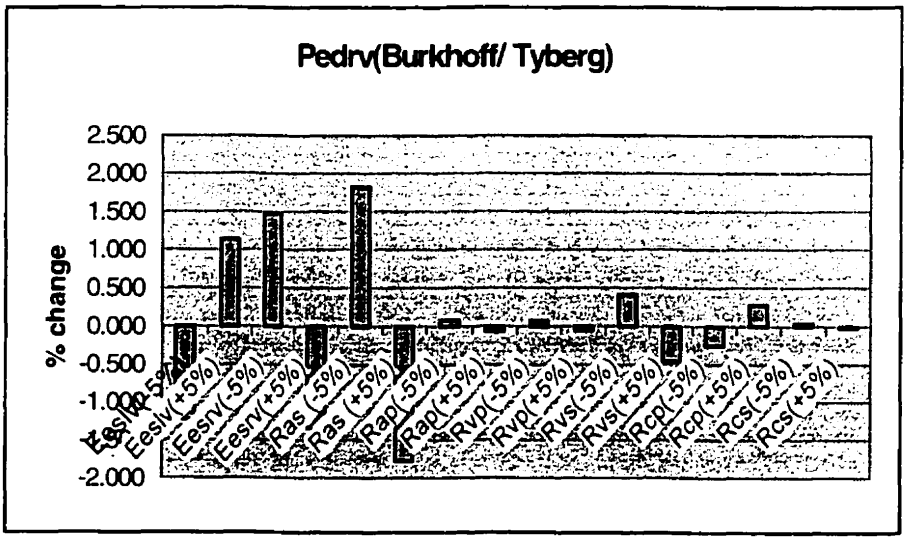
Pedrv(Burkhoff/ Tyberg)
% change
2.500
2.000
1.500
1.000
0.500
0.000
-0.500
-1.000
-2.000
Eesv(+5%)
Eesv(-5%)
Ras (+5%)
Ras (-5%)
Rap(+5%)
Rap(-5%)
Rvp(+5%)
Rvp(-5%)
Rvs(+5%)
Rvs(-5%)
Rcp(+5%)
Rcp(-5%)
Rcs(+5%)
Rcs(-5%)

Model

The plots below are charts representing the percent change in CO, MAP, PVP, PVS, Pedrv respectively with +/-5% changes in each parameter in turn.

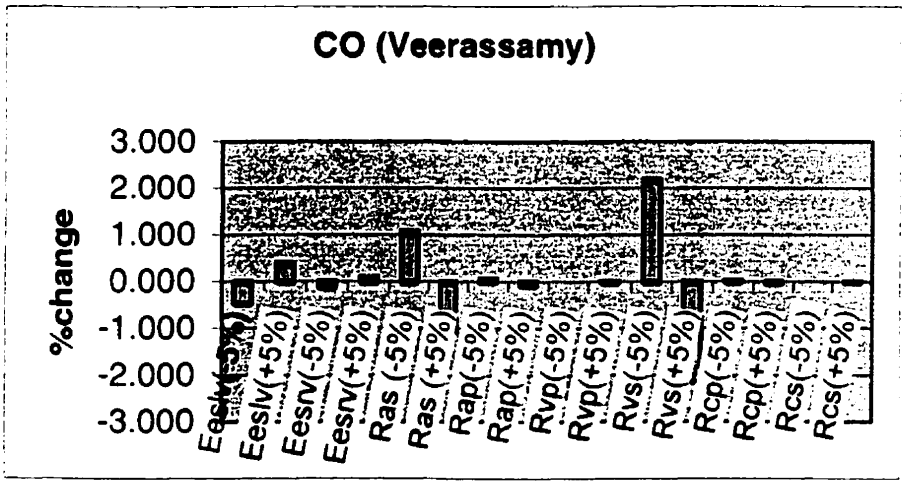

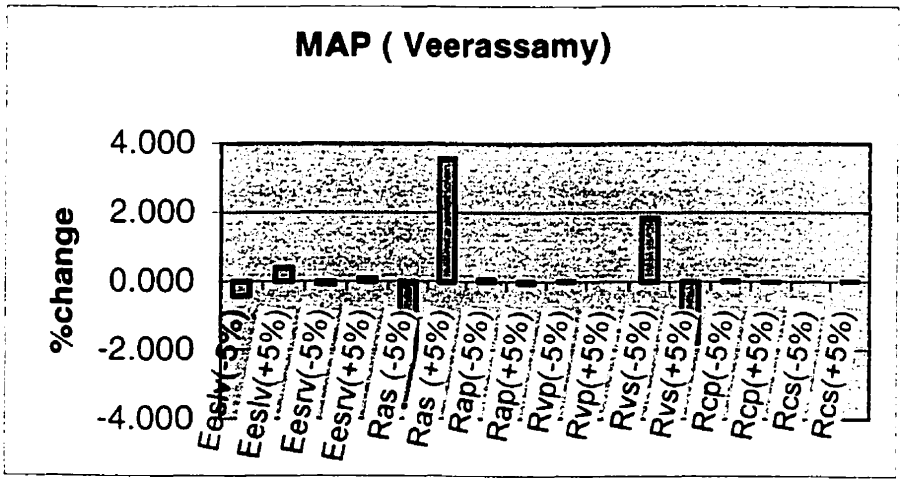

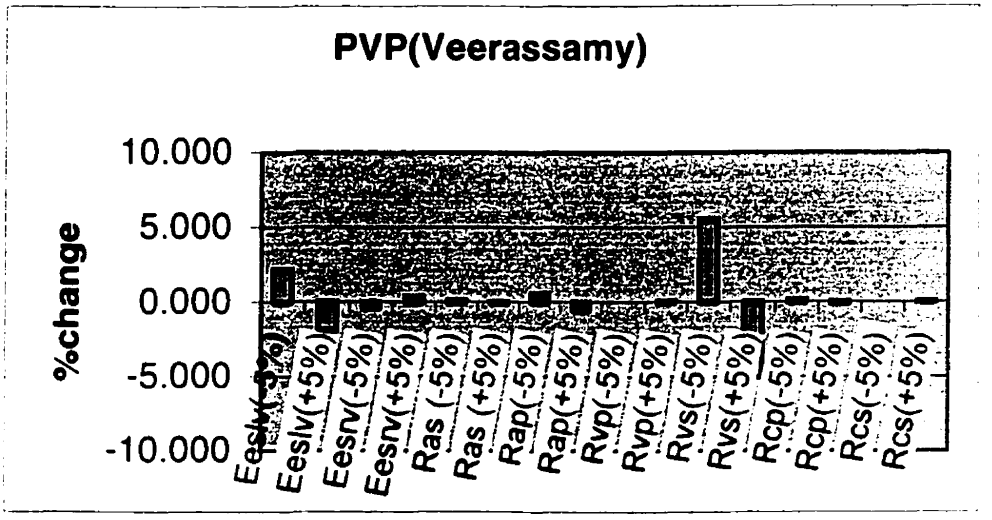
PVP(Veerassamy)
%change
10.000
5.000
0.000
-5.000
-10.000
Eeslv(-5%)
Eeslv(+5%)
Eesrv(-5%)
Eesrv(+5%)
Ras (-5%)
Ras (+5%)
Rap(-5%)
Rap(+5%)
Rvp(-5%)
Rvp(+5%)
Rvs(-5%)
Rvs(+5%)
Rcp(-5%)
Rcp(+5%)
Rcs(-5%)
Rcs(+5%)

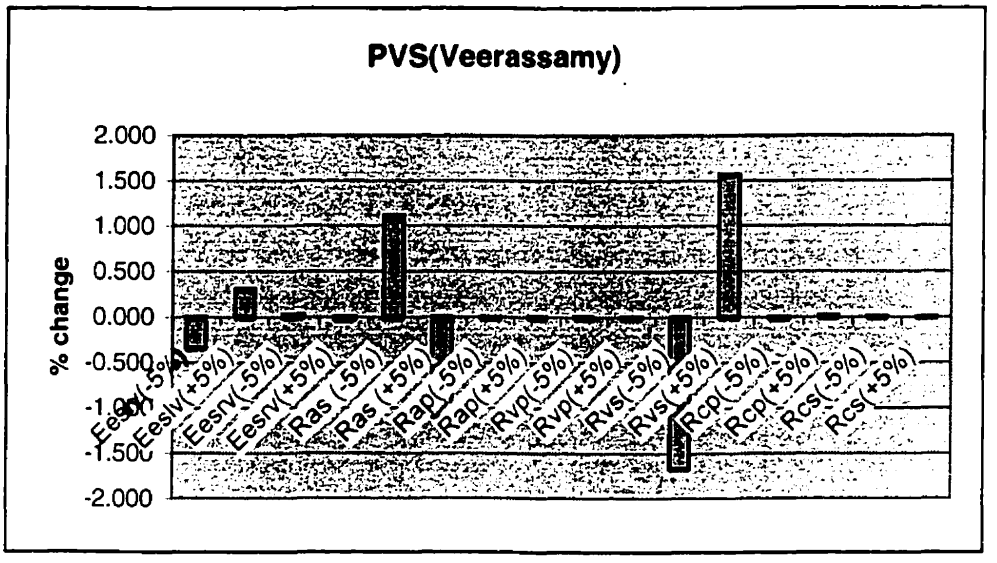
PVS(Veerassamy)
% change
2.000
1.500
1.000
0.500
0.000
-0.500
-1.000
-1.500
-2.000
Eeslv(-5%)
Eeslv(+5%)
Eesrv(-5%)
Eesrv(+5%)
Ras (-5%)
Ras (+5%)
Rap(-5%)
Rap(+5%)
Rvp(-5%)
Rvp(+5%)
Rvs(-5%)
Rvs(+5%)
Rcp(-5%)
Rcp(+5%)
Rcs(-5%)
Rcs(+5%)

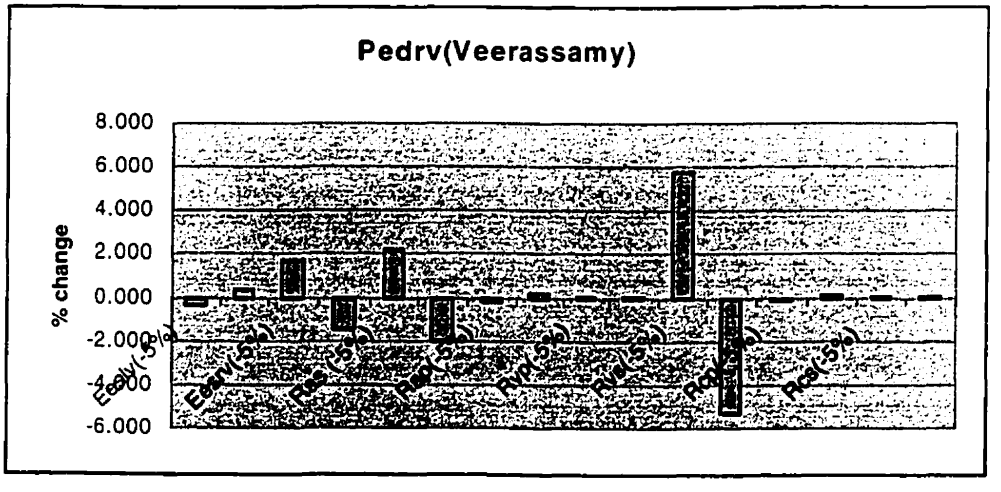
Pedrv(Veerassamy)
% change
8.000
6.000
4.000
2.000
0.000
-2.000
-4.000
-6.000
Eesrv(-5%)
Ras (-5%)
Rap(-5%)
Rvp(-5%)
Rvs(-5%)
Rcp(-5%)
Rcs(-5%)

5.3 Simulations

5.3.1 Impact of changing LV end –systolic elastance (Eeslv)

The purpose of this test was to examine the hemodynamic responses to a primary decrease in LV contractile strength with all other cardiovascular properties kept constant. As seen from figure (15) on page 67, Eeslv was varied from 6 mmHg to 0.5 mmHg/ml with control at 4mmHg/ml. As Eeslv was decreased from 4mmHg/ml to 1 mmHg/ml (representative of reduction in contractile performance) there was a substantial decrease in CO and MAP from 5.05 to 3.67 L/min and 90.01 to 66.11 mmHg. On the other hand, PVP increased from 9.64 mmHg to 23.8 mmHg.

The same test was performed taking into consideration pericardial effects (see section 4.1.4). The results obtained are a decrease in CO and MAP from 5.3 to 3.8 L/min and from 95 to 67.7 mmHg respectively. An increase in PVP is also noted in this case from 10.9 to 26.6 mmHg.

Burkhoff and Tyberg showed that reducing the contractile performance of the left ventricle had little effect on PVP. On the other hand, the results obtained in this research project demonstrates clearly that, although CO does not decrease by a substantial amount when Eeslv is halved, PVP does undergo a huge increase. The probable reason underlying why Burkhoff and Tyberg obtained a small rise in PVP is due to the smaller Mean Circulatory Filling Pressure used in their model.

5.3.2 Impact of changing Systemic Arterial resistance

The role of increasing systemic resistance in pulmonary edema was tested by setting Eeslv at half its control value (2 mmHg/ml). Ras was increased from 1.0005 to 5.29 mmHg.s/ml, resulting in a decrease in CO from 4.59 to 2.06 l/min, and an increase in MAP and PVP from 82.07 to 183.56 mmHg and from 14.07 to 20.74 mmHg respectively.

The same test was performed taking into consideration pericardial effects (see section 4.1.4). The results were obtained are a decrease in CO from 4.78 to 2.09 L/min and an increase in MAP and PVP from 84.8 to 186.74 mmHg and from 15.9 to 22.3 mmHg respectively. (Figure 16 on page 68)

Unlike the results obtained in the Burkhoff and Tyberg model, PVP is found to be sensitive to marked elevations in Ras, particularly when including the pericardial effects.

5.3.3 Impact of changing HR

In order to increase HR, Tes was decreased as HR was increased and Eeslv was set to half its control value. The results can be seen in figure (17) on page 69. CO increased from 3.8 to 5.24 l/min as HR increased from 50 to 250 beats/min and then plateaued after 150 beats/min. MAP also increased from 69.192 to 95.32 mmHg, and then plateaued. PVP decreased substantially from 20.01mmHg to 6.5 mmHg.

Similar results were obtained with the addition of the pericardial effect. CO and MAP increased from 3.98 to 5.32 l/min and 71.43 to 96.63 mmHg respectively and then both plateaued. PVP fell from 23.14 to 6.67 mmHg.

The results obtained in this analysis were similar to those obtained by Burkhoff and Tyberg although PVP was noted to have a more dramatic effect.

5.3.4 Impact of increasing stressed volume

Eeslv was set to half its normal value. The results are shown in figure (18) on page 70. On increasing Vs, CO and MAP increased from 4.5 to 6.1 l/min (at a stressed volume of about 4000ml) and from 82.1 to 112.4 mmHg respectively. The important finding, however, was a marked increase in PVP from 14.1 to 60 mmHg. This increased further as stressed volume was increased.

On adding the pericardial effect, CO and MAP increased from 4.79 to 6 l/min (at a stressed volume of about 4000ml) and from 84.9 to 110.3 mmHg respectively. As expected, PVP increased from 15.9 to 40 mmHg and then plateaued.

The results obtained from this analysis are in accordance with those obtained by Burkhoff and Tyberg in that increasing Stressed Volume has the most dramatic impact on the rise in PVP after LVD. However from the results obtained here we also note that adding the pericardial effect is very important since it acts as a limiting factor on the rise of PVP.

5.3.5 Impact of increasing Systemic Venous Resistance

This test consisted of varying Systemic Venous Resistance (Rvs) and observing the effects on CO, MAP and PVP. Rvs was varied between 0.02 and 0.8 mmHg.s/ml. CO, PVP and MAP decreased from 5.67 to 0.66 l/min, 28.19 to 0.98 mmHg and 96.8 to 25.6 mmHg, respectively.

Keeping Eeslv at half its control, Rvs was varied within the same range but with the added pericardial effect. Once more CO, PVP and MAP decreased from 5.79 to 0.67 l/min, 30.46 to 0.98 mmHg and 98.33 to 25.66 mmHg respectively. (Figure (19) on page 71)

5.4 Effect of Peripheral resistance on Model

Burkhoff/Tyberg control parameters

Eeslv	3 mmHg/ml	**Cap**	13 ml/mmHg
Eesrv	0.7 mmHg/ml	**Cas**	1.32 ml/mmHg
Ras	0.936 mmHg.s/ml	**Cvp**	8 ml/mmHg
Rap	0.0312 mmHg.s/ml	**Cvs**	70 ml/mmHg
Rvs	0.0156 mmHg.s/ml	**Stressed volume**	750 ml
Rvp	0.0156 mmHg.s/ml		
Rcs	0.021 mmHg.s/ml		
Rcp	0.0312 mmHg.s/ml		

	CO	Pedrv (Pra)	MAP	PVS	PVP
Control (Burkhoff/ Tyberg)	***5.09***	***2.58***	***76.55***	***3.80***	***13.07***
Rvs(x1/2)	5.25	2.85	78.23	3.39	14.13
Rvs(x2)	4.64	1.95	71.22	4.87	10.37

Table (4) Representation of simulation values obtained from Burkhoff/Tyberg's model

	CO	PVP	MAP	PVS[1]	Static[2] PVS	PAP	Pedrv	Pedlv
Control(Veerassamy)	***5.05***	***9.64***	***90.01***	***8.47***	***10.48***	***14.83***	***1.83***	***7.01***
Rvs(x1/2)	6.25	17.48	107.58	6.62	9.10	24.03	3.44	14.38
Rvs(x2)	3.49	4.58	66.48	10.07	11.49	8.09	0.81	2.63
Rvs(x1/2) baroreceptor reflex	6.59	17.76	90.01	7.09	9.04	24.68	3.92	14.51
Rvs(x2) baroreceptor reflex	3.22	4.68	90.03	9.36	11.47	7.92	0.72	2.86
Sepsis	5.72	11.02	70.02	8.81	10.22	16.98	0.71	8.11
Rvs(x1/2)sepsis	6.97	17.98	70.00	7.63	8.98	25.33	4.50	14.59
Rvs(x2)sepsis	3.45	4.60	70.01	9.97	11.49	8.07	0.79	2.66

Table (5) Representation of simulation values obtained from Model.

1. When Rvs was halved, CO increased more significantly in our model from 5.05 to 6.25 compared to 5.09 to 5.25 in the Burkhoff and Tyberg model.

[1] PVS is the actual value calculated under flow conditions.
[2] Static PVS is the quotient of the total stressed volume and the compliance of the vasculature (the x-intercept of the venous return curve is at zero flow).

2. When Rvs was doubled, CO decreased more substantially from 5.05 to 3.49 l/min in our model compared to 5.09 to 4.64 l/min in the Burkhoff and Tyberg model.

The next step in this test was to incorporate the baroreceptor reflex. The arterial baroreceptor reflex system is one of the most powerful and rapidly acting mechanisms for controlling arterial pressure. The rapid resetting of arterial baroreceptor afferents toward any sustained new level of blood pressure ensures that the reflex acts as an effective buffer of the short-term blood pressure fluctuations that accompany daily life. The primary purpose of the arterial baroreflex is to provide rapid and efficient stabilization of arterial blood pressure on a beat-to-beat basis by means of carotid and aortic baroreceptors. This was done in our model by maintaining the MAP constant at 90 mmHg by adjusting Ras. When Rvs is halved, CO is increased from 5.05 to 6.59 l/min in the revised model. When Rvs is doubled CO is decreased from 5.05 to 3.22 l/min in the revised model.

The last step in this test was to induce sepsis and see the consequences on Cardiac Output when peripheral resistance was perturbed. Sepsis (shock) is a progressive, widespread reduction in tissue perfusion that results from a decrease in effective circulating blood volume causing a decrease in oxygen delivery and/or exchange in the capillary circuit. Shock is a cyclic, self-perpetuating problem with numerous causes, all of which feature poor perfusion, anaerobic metabolism and release of tissue damaging mediators. During sepsis, MAP drops due to the decrease in mean systemic filling pressure.

Our approach was to allow MAP to drop to 70 mmHg, again by adjusting Ras. Once again, as expected similar but more drastic effects are obtained. CO increased from 5.05 to 6.97 l/min when Rvs was halved. CO decreased from 5.05 to 3.45 l/min when Rvs was doubled.

These results match those determined experimentally by Madger [24].

Figure (15) Impact of changing LV End-systolic elastance

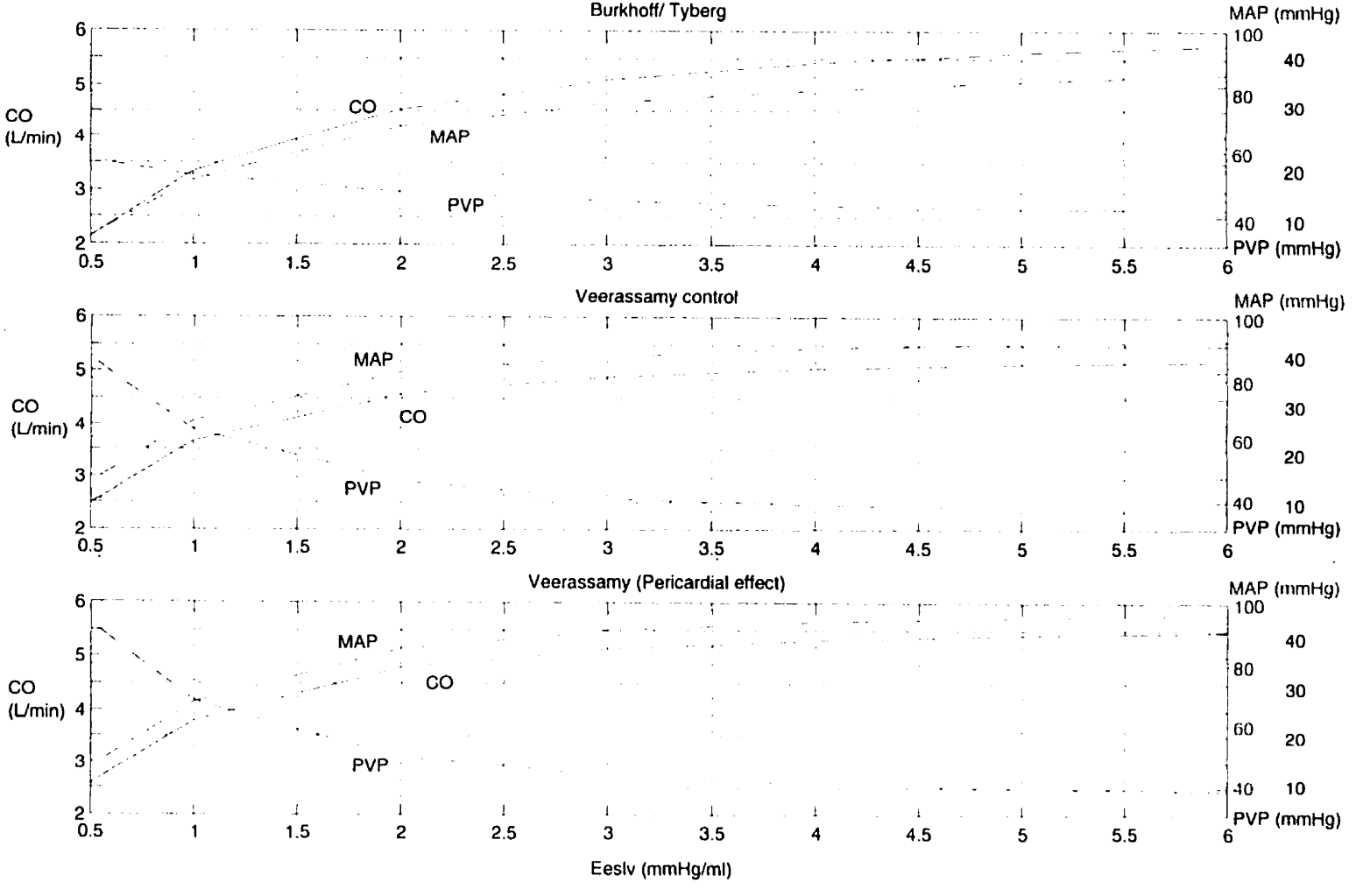

Figure (16) Impact of changing Systemic Arterial Resistance with LV end systolic elastance at half control

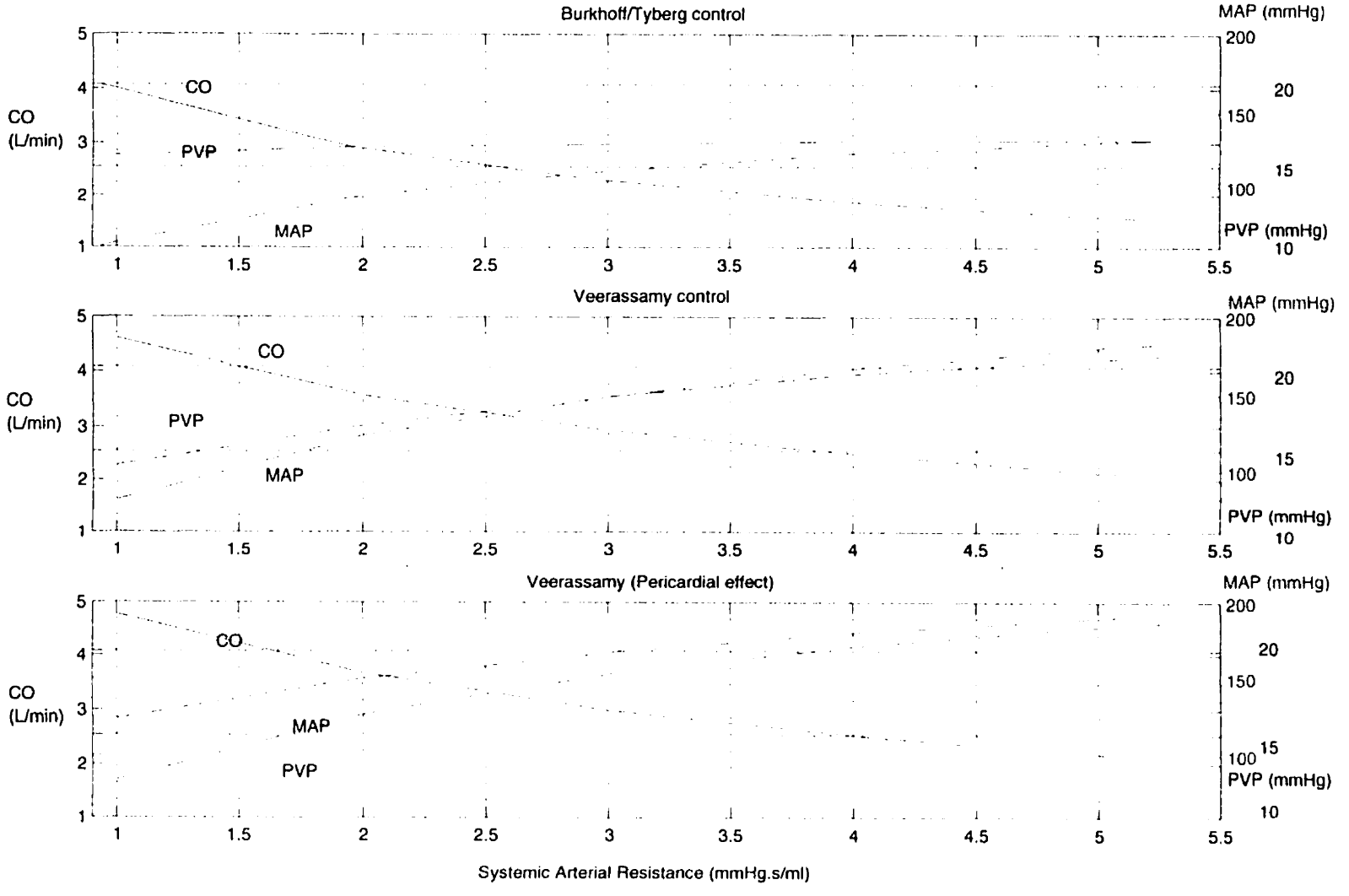

Figure (17) Impact of changing Heart Rate with LV end-systolic elastance at half its control

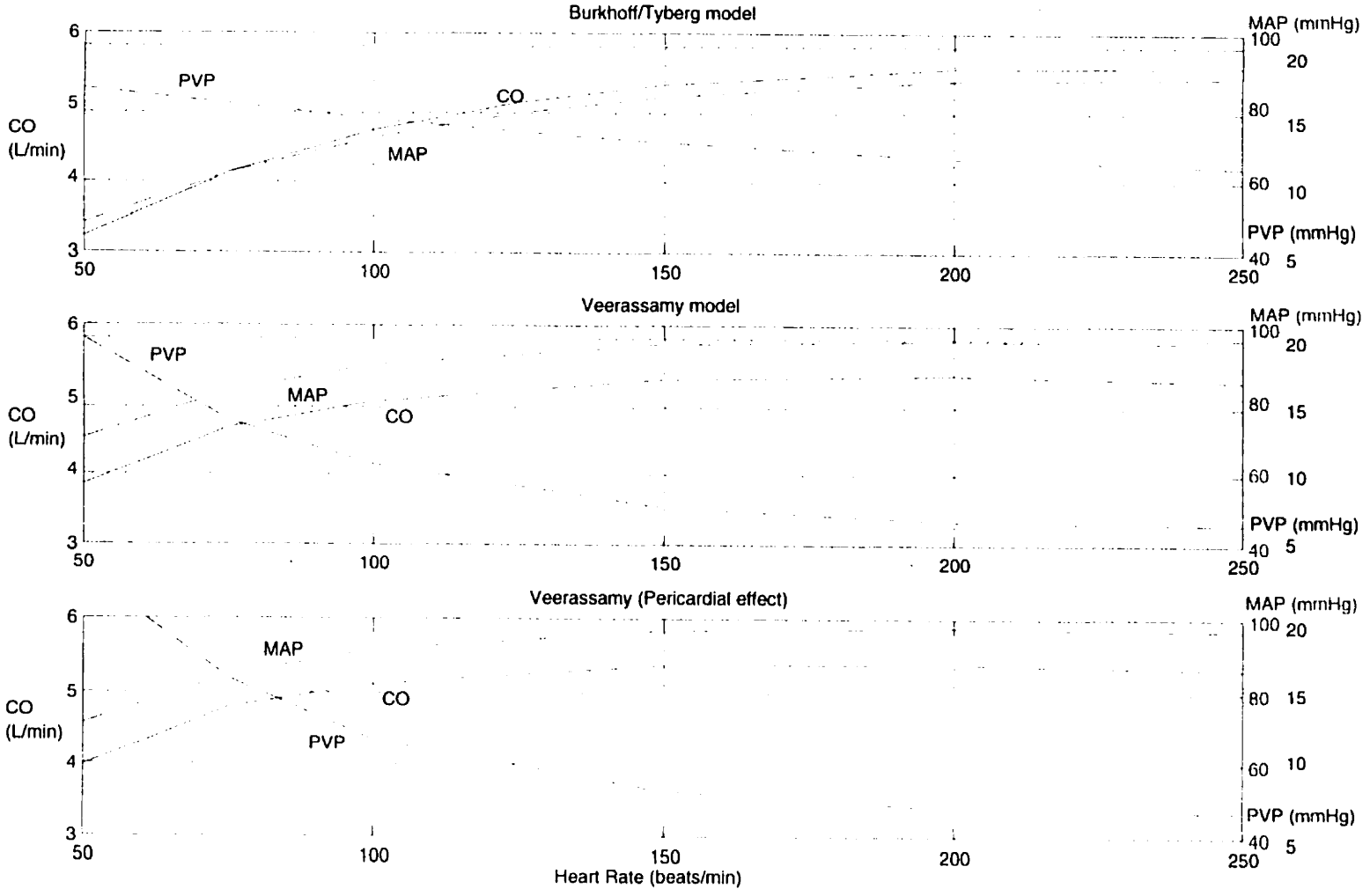

Figure (18) Impact of Stressed Volume with LV end-systolic elastance at half its control

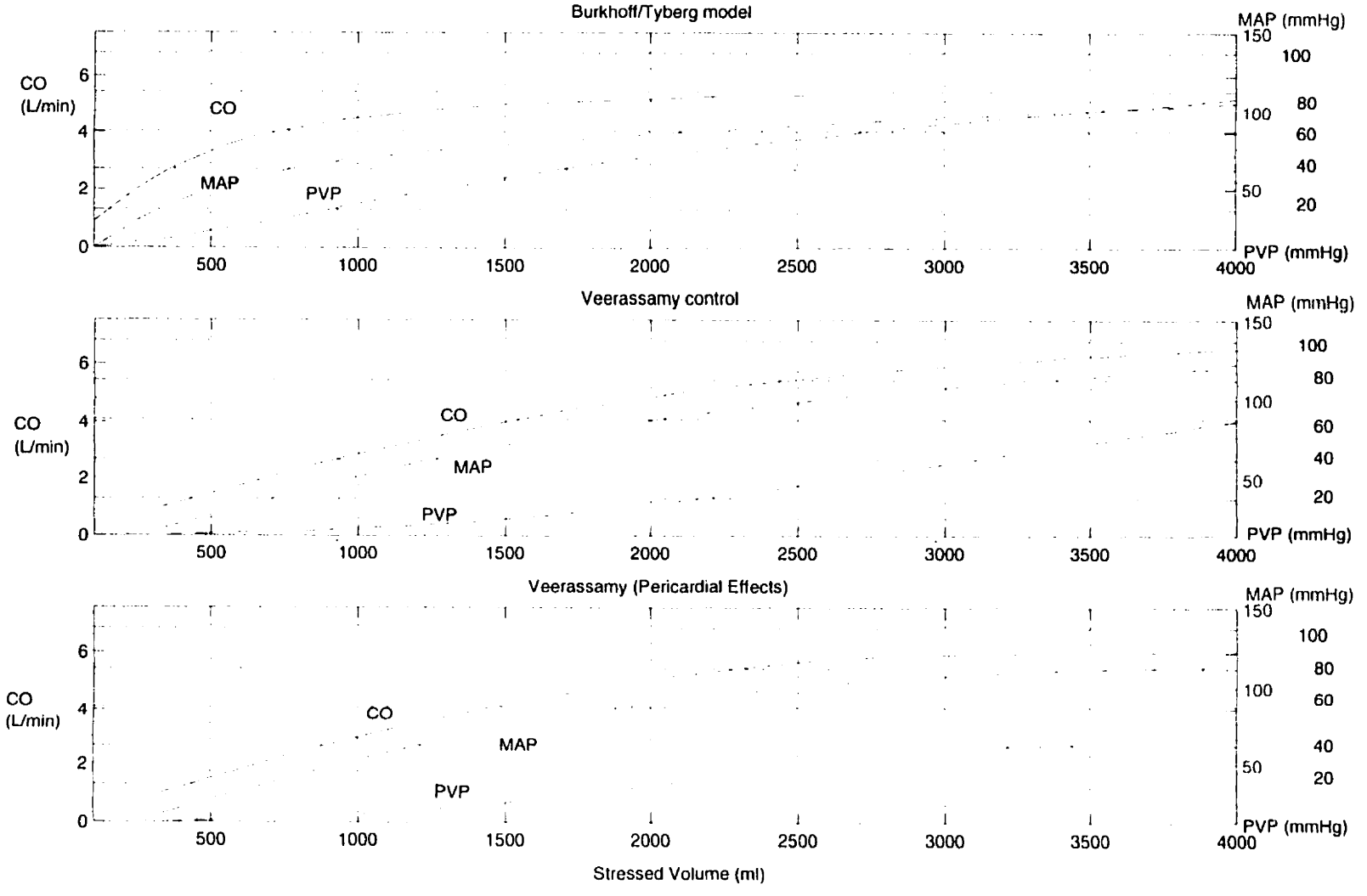

Figure (19) Impact of changing Systemic Venous Resistance with LV end systolic elastance at half its control

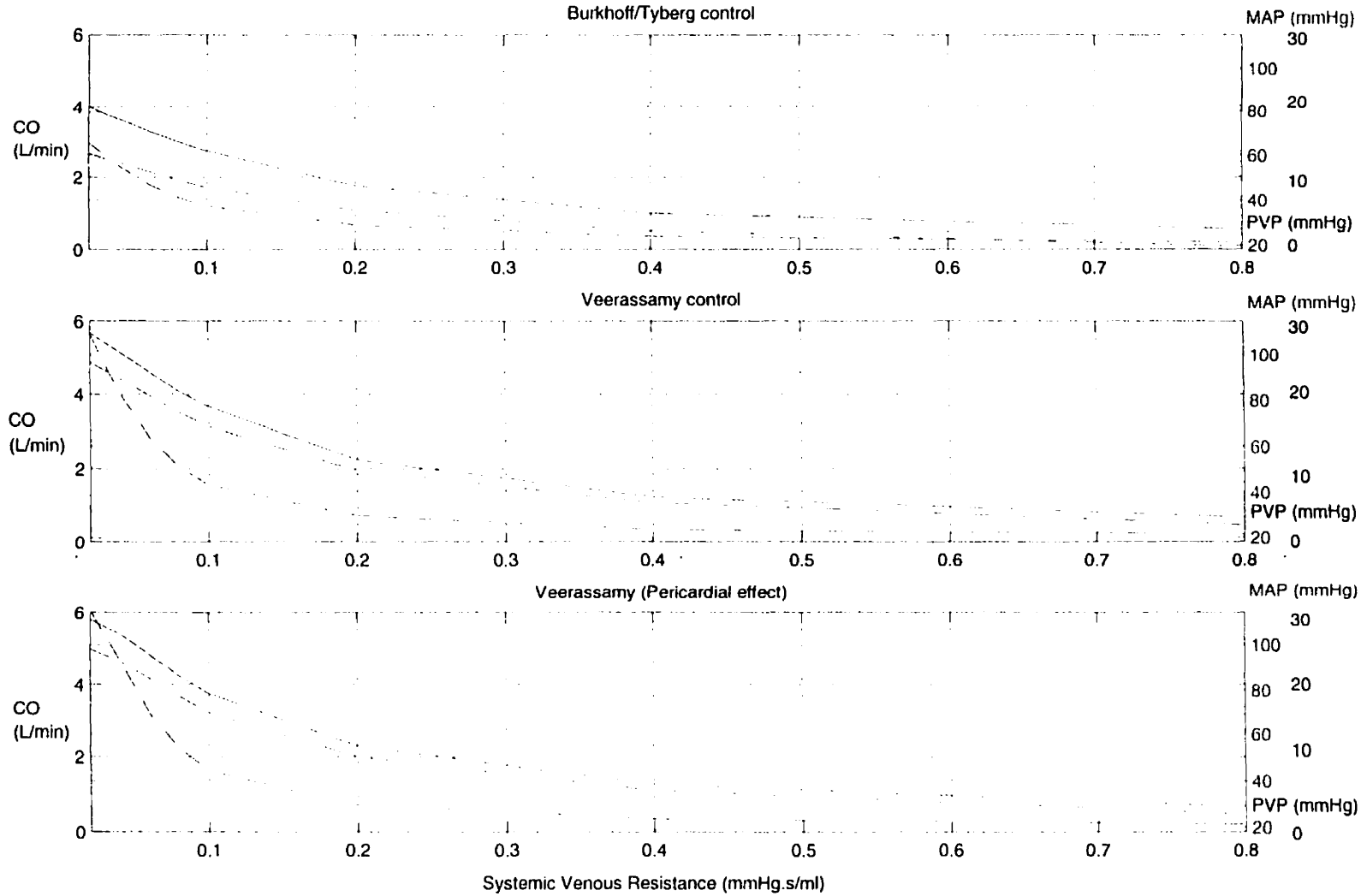

5.5 DISCUSSION

The results obtained from this analysis clearly suggest that significant rises of PVP do occur as a consequence of acute LVD. On decreasing LV strength (decreasing Eeslv), MAP (blood pressure) and cardiac output were decreased and PVP was increased whereas in the Burkhoff and Tyberg model there was only minimal increase in PVP. Increases in systemic arterial resistance caused a rise in blood pressure, a decrease in cardiac output and a rise in PVP. Increasing heart rate had a role in restoring cardiac output, but caused a significant decrease in PVP. An increase in stressed volume caused an increase in CO which eventually plateaued, a rise in blood pressure and a rise in PVP.

The results obtained are unlike those from Burkhoff and Tyberg who concluded that stressed vascular volume is the only quantity capable of elevating PVP substantially. This analysis shows clearly that although stressed volume produces a rise in PVP so does decreasing LV strength and increasing systemic arterial resistance.

Adding the pericardial effect caused CO to plateau earlier and a smaller rise in MAP. A smaller but still notable rise in PVP also occurred. The pericardial effect thus attenuated the effects of increasing stressed volume. This leads to the conclusion that the pericardium acts as a limiting factor in the rise of PVP after the onset of acute LVD.

Our model's behaviour was generally consistent with both clinical and experimental observations [12, 13, 14, and 24]. The results obtained in this analysis are in agreement

with the commonly held notion that LV function leads to a primary increase in ventricular end-diastolic pressure that is transmitted backward to the pulmonary venous system (unlike that faced by Burkhoff and Tyberg). In addition, they are consistent with the notion that impaired LV function leads to a primary increase in PVP due to blood shifting to the pulmonary from the systemic system.

The validity of our choice of parameters and their ratios in the revised model is reinforced by the results of changing systemic venous resistance. Compared to the results obtained with the original model of Burkhoff and Tyberg, we obtained a bigger rise in cardiac output. On addition of the baroreceptor reflex (reflecting more appropriately the human system), an even larger rise in cardiac output was obtained and this was further elevated in the case of sepsis. In addition, these results are consistent with those obtained in humans.

In order to ascertain the validity of our model in this project, a comparison of our results was made with previous work done in this area. A current understanding of the dynamics of the closed-loop circulatory system is mainly based on the theoretical and experimental work of Guyton and his colleagues. Their studies explained why the venous pressure-volume curve shifts downward and to the left during acute heart failure. This is attributed to the shifting of blood from the systemic to the pulmonary systems due to the transient mismatch of stroke volumes between the right and left ventricles. The underlying mechanism in our model regarding the accumulation of blood in the pulmonary circulation is similar to that of Guyton but different from that of Burkhoff and Tyberg. The conclusion derived from the present project, which matches Guyton et al., is that the

transient stroke volume mismatch is a direct consequence of the sudden decrease in LV contractile strength. Burkhoff and Tyberg's conclusion, however, is that accumulation of blood in the pulmonary circuit is primarily due to redistribution of blood from the unstressed to the stressed pool. From our results we can thus conclude that whereas increased stressed volume after the onset of LVD is definitely a key factor in raising PVP, it is not the only one. The other factors include changes in left ventricular end-systolic elastance, systemic arterial resistance and heart rate.

To further reinforce our model, the sensitivity analysis given in section 5.2 shows that a crucial factor is the right choice of parameter values and their ratios. This sensitivity analysis clearly shows the differences between the Burkhoff and Tyberg model and the one described in this thesis. Our most significant observation here is the percent change in cardiac output when Rvs is perturbed. In the normal human, a change in Rvs is expected to cause a change in pumping effectiveness and hence cardiac output. This change is hardly noticeable in the Burkhoff and Tyberg model. Furthermore, as predicted, on addition of the baroreceptor reflex and sepsis, bigger increases in cardiac output were observed in our model. Indeed, such effects can be inferred by inspection of the model. (Eq.4.1-4.10)

	CO	MAP	PVP
Eeslv (↓)	(↑)	(↑)	(↓)
Eeslv(↓) (with pericardial effect)	(↑)	(↑)	(↓)
HR (↑)	(↑)	(↑)	(↓)
HR(↑) (with pericardial effect)	(↑)	(↑)	(↓)
Ras (↑)	(↓)	(↑)	(↑)
Ras (↑) (with pericardial effect)	(↓)	(↑)	(↑)
Stressed Volume (↑)	(↑)	(↑)	(↑)
Stressed Vol.(with pericardial effect)	(↑)	(↑)	(↑)

Table (6): Summary of simulations

CHAPTER 6

CONCLUSIONS AND SUGGESTIONS FOR FUTURE RESEARCH

6.1 Limitations of the model

The model described in this project deals with the circulatory system at the macroscopic level. The added compartments are lumped, and not all neurohumoral control mechanisms are taken into account. Care is taken in choosing the parameters and those were based on experimental values obtained by Magder [24]. Despite the relative simplicity, this model of the cardiovascular system behaves in a manner consistent with clinical and experimental observations in almost every way.

This model does not include the atria. Atrial contraction enhances ventricular filling so that ventricular end-diastolic pressure may be greater than PVP at high heart rates. But, relatively substantial increases in left ventricular filling pressure is ineffective at raising ventricular diastolic volume, due to the impact of the pericardial constraints. It is therefore predicted that the impact of the atria on amplifying cardiac output or lessening the degree of pulmonary congestion would be minimal. [7]

We assume that blood volume remains constant after venoconstriction. However fluid can shift to the extravascular from the intravascular space when venous pressure rises. It has been argued though that the degree to which this effect can alter blood volume is small. [7]

6.2 Applications and suggestions for future research

(1) This model is relatively easy to understand and use. One of its applications could therefore be as an educational tool for Medical Students studying hemodynamics.

(2) Clinical scenarios other than LVD could be investigated, such as sepsis and heart failure.

(3) A parallel venous compartment could be added to represent the splanchnic system. The aim would be to investigate the impact of changes of peripheral arterial resistance and splanchnic arterial resistance on CO.

6.3 Summary and Conclusions

This thesis describes a modified version of the cardiovascular model of Burkhoff and Tyberg [7]. The key modifications include changes in the values of resistance and compliance. Stressed vascular volume and elastance parameters were also adjusted so as to have the model be representative of the human system. The simulations performed by Burkhoff and Tyberg were repeated and the effects of the pericardium were also investigated, along with the effects of changes in the systemic venous resistance. A sensitivity analysis was performed on each parameter by perturbing independently of the other parameters and then observing its effects on the system.

The results obtained show that PVP is increased after the onset of LVD as a consequence not only of changes in stressed volume but also changes in contractile strength, systemic arterial resistance and heart rate. Whereas increasing stressed volume raised PVP from 14.1 to 60 mmHg, contractile strength raised PVP from 9.64 to 23.8 mmHg and systemic

arterial resistance increased PVP from 14.07 to 20.74 mmHg. (Figures 18, 15, 16 respectively). It was shown that the pericardium acts a limiting factor in the rise of PVP after LVD. With the addition of the pericardial effects, as stressed volume was being increased, PVP increased from 15.9 to 40 mmHg and then plateaued (Figure (18)).

This sensitivity analysis confirmed that the choice of the parameter values and their ratios used in our model are more appropriate than those used by Burkhoff and Tyberg. Our model was also found to be consistent with both clinical and experimental observations made by Dr. S. Magder [24].

APPENDICES

APPENDIX 1: DICTIONARY LISTINGS (definitions)

Terms (Alphabetical order)	Definition
Arteries	Vessels that carry blood from the left to the right ventricles to the tissues.
Blood	Suspension of cells in fluid plasma. Its components are erythrocytes (RBCs), leukocytes (white cells) and platelets (thrombocytes). The average number is approximately $5*10^6$, 10^4 and $3*10^5$ for each per mm cube, respectively.
Capillary	Finest blood vessels, about 5-6 um in diameter and 0.5 mm in length in the systemic circulation
Cardiac Output	CO (l/min)= Stroke Volume x Heart rate
Compliance	A measure of the ability of a hollow structure to change its volume. P=V/C (ml/mmHg)
Diastole (Atrial or Ventricular)	Resting phase of cardiac cycle
Ejection Fraction	EF = Stroke Volume/ End-diastolic LV volume
Elastance	reciprocal of compliance (mmHg/ml)
Heart	Mammalian heart is made up of 4 chambers namely the right and left atria and the right and left ventricles. The auricles are thin walled chambers into which blood flows from the veins at low pressure. Between the auricles and ventricles are valves namely the tricuspid (right) and mitral (left). Blood flows out of the ventricles past the valves into the pulmonary artery (right) and aorta (left). Both auricles beat simultaneously shortly before the synchronous beat of the ventricles.
Inertia	Represented by the property of density and is the force needed to accelerate fluid

	particles, provided by a pressure gradient.
Laminar flow	Refers to the fluid velocity, which remains constant on cylindrical surfaces within the fluid, which are concentric with the axis. The flow is ordered, stable and can be considered as individual cylindrical laminae of fluid sliding over each other.
Mean Arterial Pressure(MAP)	MAP =Pd +[1/3*(Ps-Pd)] where Pd is diastolic arterial pressure and Ps is Systolic arterial pressure
Mean Circulatory Filling Pressure	Pressure measured at all pt. in the circulatory system if the heart were stopped suddenly. In this model, it is approximated as mean systemic pressure, Pms or Pvs.
Peripheral resistance	Ratio of the mean pressure drop across a circulatory bed to the mean flow through it. (mmHg.s/ml)
Pressure	Measure of force per unit area exerted by a fluid (mmHg)
Pressure gradient	pressure drop per unit length along a flow channel
Stressed blood volume	Blood driven through the vasculature. In this project only stressed volume is present. (ml)
Stroke Volume	Amount of blood pumped out per beat (ml). Stroke Vol. = Volume – End –systolic LV Volume
Systemic circulation	Circulation to body excluding the pulmonary circulation
Systole (Atrial or Ventricular)	Active part of cardiac cycle
Turbulence	Characterized by random fluctuations of the fluid motions, which cannot be predicted in detail. The flow is usually unstable.
Unstressed blood volume	also known as dead volume that can be placed in a capacitive vessel without

	raising its pressure above 0mmHg
Veins	Vessels carrying blood from the tissues to the atria of the heart.
Viscoelasticity	Material in which both the strain and rate of strain are functions of the imposed stress.
Viscosity	Property of resisting deformation in a fluid. (Poise)
Windkessel	Term used by Otto Frank (1899) to describe the elastic reservoir function of the aorta. The systemic bed was modeled as an elastic reservoir connected to a peripheral hydraulic resistance in the simple windkessel theory.

APPENDIX 2: LIST OF SYMBOLS, SUBSCRIPTS, UNITS EMPLOYED

Symbols	Terms	Units
Eeslv	End systolic LV elastance	mmHg/ml
Eesrv	End systolic LV elastance	mmHg/ml
Ras	Resistance systemic artery	mmHg.s/ml
Rap	Resistance pulmonary artery	mmHg.s/ml
Rvp	Resistance pulmonary vein	mmHg.s/ml
Cap	Compliance in pulmonary artery	ml/mmHg
Cas	Compliance in pulmonary artery	ml/mmHg
Cvs	Compliance in systemic vein	ml/mmHg
Cvp	Compliance in pulmonary vein	ml/mmHg
Alv, Arv	Scaling factor for EDPVR	mmHg
Blv, Brv	Exponent for EDPVR	1/ml
Tes	Time to end systole	ms
Tau (τ)	Time constant of relaxation	ms
Vs	Stressed Volume	ml
HR	Heart Rate	Beats/min
SV	Stroke Volume	ml
CO	Cardiac Output	L/min
Pressures		
MAP	Mean Arterial Pressure	mmHg
Pas	Systemic Arterial pressure	mmHg
PVS (Pvs)	Systemic Venous pressure	mmHg
Pedlv	End-diastolic LV pressure	mmHg
Pedrv	End-diastolic RV	mmHg

	pressure	
Plv	Left ventricular pressure	mmHg
Prv	Right ventricular pressure	mmHg
PVP (Pvp)	Pulmonary venous pressure	mmHg
Pap	Pulmonary arterial pressure	mmHg
Volumes		
Vlv	LV volume	ml
Vrv	RV volume	ml
Vap	Pul. Arterial vol.	ml
Vas	Systemic Arterial vol.	ml
Vvs	Systemic venous vol.	ml
Vvp	Pul. venous vol.	ml
Flows		
dVlv	Left ventricular flow	--
dVrv	Right ventricular flow	--
dVas	Systemic Arterial flow	--
dVap	Pulmonary arterial flow	--
dVvp	Pulmonary venous flow	--
dVvs	Systemic venous flow	--
a-	Elastance	
c	Compliance	
F	Flow	
g	Gravitational acceleration	
l	Length	
L	Inertance	
n	Number of g acceleration	
P	pressure	
R	resistance	
t	time	
t_c	Time elapsed	
T	period	
V	Volume	

i,j,k	Segmental subscripts	
x,y,z	Periodic elastic functions	
	Venous collapse parameter	
	Venous retrograde flow parameter	
	Density	
	Time constant	

REFERENCES:

[1] Atkins G.L, "Multi-compartmental Models in Biological Systems", London: Methuen, 1969.

[2] Berne, R .M., Levy, H.N, "Cardiovascular Physiology", St. Louis: Mosby, 1997.

[3] Bergel D.H, "Cardiovascular Fluid Dynamics", London, New York, Academic Press, 1972.

[4] Beneken J.E.W and De Wit B, " A Physical approach to hemodynamic aspects of the human cardiovascular system", 1967.

[5] Luetscher J. A, Boyers D. G, Cuthbertson J.G, McMahon D.F, "A model of the human circulation. Regulation by autonomic nervous system and renin-angiotensin system, and influence of blood volume on cardiac output and blood pressure." Circulation Research. 32:Suppl 1:84-98, 1973.

[6] Bronzino, " The Biomedical Engineering Handbook", IEEE Press, 2386-2400, 1997.

[7] Burkhoff D, Tyberg J, "Why does pulmonary venous pressure rise after onset of LV dysfunction: a theoretical analysis" Am. J. Physiol. 265 H1819-H1828, 1993

[8] Constantinescu V.N, "Laminar Viscous Flow", New York: Springer, 1995.

[9] Dick, D., E. and Kendrick, J. E., Matson, G. L., RideOut, V. C., "Measurement of non-linearity in the arterial system of the dog by a new method", Circ. Res. 22, 101-111, 1968

[10] Erwin, F., Idelchik, I.E," Flow resistance -A Design Guide for Engineers", NewYork: Hemisphere Pub. Co, 1989.

[11] Fardipour P, "Computer modeling of the cardiovascular system based on relational analysis" Ph.D. Thesis from City University, 1989.

[12] Fitz-Gerald J.M, " The Mechanics of Capillary Blood Flow" In "Cardiovascular Fluid Dynamics", New York, Academic Press, 1972.

[13] Green J, F, "Fundamental cardiovascular and pulmonary physiology", Philadelphia: Lea & Febiger, 1987.

[14] Guyton, A. C, " Determination of cardiac output by equating venous return curves with cardiac response curves" Physiol. Rev., 35, 123-129, 1955

[15] Guyton A.C, " Circulation Physiology: Cardiac Output and Its Regulation", Philadelphia, Saunders, 1973.

[16] Grodins, F., S., "Interactive cardiovascular physiology: a mathematical synthesis of cardiac and blood vessel hemodynamics", Quart. Rev. Biol., 34, 93-116, 1959

[17] Harreveld, A. Van, Feigen, G. A., Lerman, L. S., 'Hemodynamics of aortic occlusion", Am. J. Physiology. , 157, 168-176, 1949.

[18] Heller L., Mohrman D.E, "Cardiovascular Physiology", New York: McGraw-Hill, 1981.

[19] Hwang N.H.C., Normann N.A," Cardiovascular Flow Dynamics", Baltimore: University Park Press 1977.

[20] Karakawa M; Igarashi K, " A Mathematical Approach to Cardiovascular Disease", Tokyo: Kokuseido Pub. Co., 1998.

[21] Leaning M. S., Pullen H.E; Carson E.R; Finkelstein L, "Modeling a complex biological system: the human cardiovascular system-1 Methodology and model description", 1983.

[22] Little R, C, " Physiology of the Heart & Circulation", Chicago: Year Book Medical Publishers, 1985.

[23] McDonald D.A, "Blood flow in arteries", London: Edward Arnold, 1974.

[24] Magder S, "Venous mechanics of contracting gastrocnemius muscle and the muscle pump theory. J.Appl. Physiol. 79: 930-1935, 1995.

[25] Naamani, R, S.N.A Hussain, S. Madger, "The mechanical effects of contractions on muscle blood flow. Eur J. Appl. Physiol. 71: 102-112, 1995.

[26] Middleman," Transport Phenomena in the cardiovascular system", N.Y.: Wiley-Interscience, 1972.

[27] Milnor W.R, " Pulmonary Hemodynamics" in "Cardiovascular Fluid Dynamics", London, New York, Academic Press, 1972.

[28] Noordergraaf, A., Verdouw, P. D., and Boom, H.B. K, "The use of an analog computer in a circulation model", Progress in Cardiovascular Diseases, 5, 419-439, 1963.

[29] Noordergraaf A, "Circulatory System Dynamics", Cambridge, Mass.: MIT Press, 1978.

[30] Oldenburger, MacMillan, "Mathematical Engineering Analysis", 1950.

[31] Piene H, Smiseth O.A, Refsum H, Tyberg J.V, " Apparent depression of right ventricular function after selective reduction of left ventricular inotropy: an interpretation of experimental data utilizing a computer- based circulatory model", Med & Biol. Eng & Comput 1983, 21, 548-556

[32] Pullen, H. E., " Studies in the Modeling and simulation of the Human Cardiovascular System with application to the effects of drugs, Ph.D. Thesis, City University, London, 1983.

[33] Rushmer R.F, " Cardiovascular Dynamics", Philadelphia: Saunders, 1976.

[34] Sagawa H, "Some computer models in Cardiovascular research" In "Cardiovascular Fluid Dynamics", London, New York, Academic Press, 1972.

[35] Sagawa K, "The ventricular pressure-volume diagram revisited", Circulation Research 43(5) Nov 1978 pp. 677-687

[36] Sandquist G M, Olsen D B, Kolff WJ, A comprehensive elementary model of the mammalian circulatory system", Annals of Biomed. Eng. 10(1): 1-33, 1982

[37] Skalak R, "Synthesis of a Complete Circulation" In "Cardiovascular Fluid Dynamics", London, New York, Academic Press. 1972.

[38] Shepherd, J.T, Vanhoutte, P. M, " The Human Cardiovascular System, facts and concepts", Raven Press, 1979.

[39] Smith J.J, Kampine J.P., " Circulatory Physiology-the essentials", Williams and Wilkins, 1990

[40] Taylor, C; Johnson, J.A; Smith, W.R, "Numerical Methods in Laminar and Turbulent Flow", Swansea: Pineridge Press, 1983.